Active shortening of the Cascadia forearc and implications for seismic hazards of the Puget Lowland

Samuel Y. Johnson,[1] Richard J. Blakely,[2] William J. Stephenson,[3] Shawn V. Dadisman,[4] and Michael A. Fisher[2]

Received 28 January 2003; revised 17 October 2003; accepted 11 November 2003; published 31 January 2004.

[1] Margin-parallel shortening of the Cascadia forearc is a consequence of oblique subduction of the Juan de Fuca plate beneath North America. Strike-slip, thrust, and oblique crustal faults beneath the densely populated Puget Lowland accommodate much of this north-south compression, resulting in large crustal earthquakes. To better understand this forearc deformation and improve earthquake hazard assessment, we here use seismic reflection surveys, coastal exposures of Pleistocene strata, potential-field data, and airborne laser swath mapping to document and interpret a significant structural boundary near the City of Tacoma. This boundary is a complex structural zone characterized by two distinct segments. The northwest trending, eastern segment, extending from Tacoma to Carr Inlet, is formed by the broad ($\sim$11.5 km), southwest dipping ($\sim$11°–20°) Rosedale monocline. This monocline raises Crescent Formation basement about 2.5 km, resulting in a moderate gravity gradient. We interpret the Rosedale monocline as a fault-bend fold, forming above a deep thrust fault. Within the Rosedale monocline, inferred Quaternary strata thin northward and form a growth triangle that is 4.1 to 6.6 km wide at its base, suggesting $\sim$2–3 mm/yr of slip on the underlying thrust. The western section of the >40-km-long, north dipping Tacoma fault, extending from Hood Canal to Carr Inlet, forms the western segment of the Tacoma basin margin. Structural relief on this portion of the basin margin may be several kilometers, resulting in steep gravity and aeromagnetic anomalies. Quaternary structural relief along the Tacoma fault is as much as 350–400 m, indicating a minimum slip rate of about 0.2 mm/yr. The inferred eastern section of the Tacoma fault (east of Carr Inlet) crosses the southern part of the Seattle uplift, has variable geometry along strike, and diminished structural relief. The Tacoma fault is regarded as a north dipping backthrust to the Seattle fault, so that slip on a master thrust fault at depth could result in movement on the Seattle fault, the Tacoma fault, or both. *INDEX TERMS:* 8107 Tectonophysics: Continental neotectonics; 8015 Structural Geology: Local crustal structure; 3025 Marine Geology and Geophysics: Marine seismics (0935); 7230 Seismology: Seismicity and seismotectonics; 8110 Tectonophysics: Continental tectonics—general (0905); *KEYWORDS:* Seattle uplift, Tacoma fault, Rosedale monocline, margin-parallel shortening. **Citation:** Johnson, S. Y., R. J. Blakely, W. J. Stephenson, S. V. Dadisman, and M. A. Fisher (2004), Active shortening of the Cascadia forearc and implications for seismic hazards of the Puget Lowland, *Tectonics*, *23*, TC1011, doi:10.1029/2003TC001507.

1. Introduction

[2] Oblique convergence of tectonic plates at subduction zones commonly leads to strain partitioning in which deformation is resolved into two components of strain [e.g. *Fitch*, 1972; *Jarrard*, 1986; *Yu et al.*, 1993; *Chemenda et al.*, 2000]. One strain component, perpendicular to the subduction zone, is accommodated by margin-parallel thrust faults (margin-normal shortening). The second strain component is parallel to the subduction zone and typically results in a broad region of oblique-slip faulting in the forearc region of the upper plate. Combined movement along thrust and strike-slip faults in the forearc can lead to the simultaneous translation and rotation of large crustal blocks. The style and geometry of strain partitioning results from the interplay among many variables such as the obliquity of the plate convergence, the dip of the subducted plate, the amount of interplate coupling, the thermal state of the subduction zone, and the structural fabric and geometry of the forearc. Strain partitioning and associated forearc deformation has been described from several oblique-convergent margins, among them Sumatra [*Fitch*, 1972; *McCaffrey et al.*, 2000b], New Guinea [*Abers and McCaffrey*, 1988], Japan [*Hashimoto and Jackson*, 1993; *Fabbri and Fournier*, 1999; *Lallemand et al.*, 1999], the Aleutians Islands [*Ave Lallemant*, 1996; *Geist et al.*, 1988], South America [*Freymueller et al.*, 1993], and Cascadia [*Wells et al.*, 1998; *McCaffrey et al.*, 2000a], which is the subject of this report.

[3] The Cascadia convergent margin is characterized by oblique subduction of the Juan de Fuca plate beneath North America. Paleomagnetic, geologic, and GPS data indicate that the Oregon portion of the Cascadia forearc, comprised largely of Eocene volcanic and overlying sedimentary

[1]U.S. Geological Survey, Santa Cruz, California, USA.
[2]U.S. Geological Survey, Menlo Park, California, USA.
[3]U.S. Geological Survey, Denver, Colorado, USA.
[4]U.S. Geological Survey, St. Petersburg, Florida, USA.

rocks, is rotating clockwise at about 1.5°/m.y. and translating northward at a rate of 6 mm/yr. Farther north in Washington, this northward migrating forearc block abuts against a relatively stationary buttress of Mesozoic and older rocks in southwestern Canada and northwestern Washington, yielding margin-parallel shortening [*Johnson et al.*, 1996; *Wells et al.*, 1998]. Our challenge in this report is to document the style and geometry of margin-parallel shortening in the densely populated Puget Lowland portion of the Cascadia forearc (Figure 1) and to address the implications of this active deformation for earthquake hazard assessment. Meeting this challenge has required integrated analysis of several data sets, including conventional and high-resolution seismic reflection profiles, potential fields surveys, geologic mapping, and airborne laser swath mapping.

[4] Crustal faults of the Puget Lowland were originally inferred on the basis of geophysical anomalies [*Danes et al.*, 1965; *Gower et al.*, 1985]). The Seattle fault, Devils Mountain fault, and southern Whidbey Island fault (Figure 1), for example, all correspond to significant linear gravity and (or) magnetic anomalies [*Finn et al.*, 1991; *Johnson et al.*, 1996, 2001; *Blakely et al.*, 2002]. Documentation of these structural zones has been difficult due to minimal exposure and to extensive cover of dense vegetation and late Pleistocene glacial and interglacial deposits.

[5] The Seattle fault forms the boundary between the Seattle uplift and Seattle basin, juxtaposing dense, highly magnetic, and high-velocity rocks to the south and less dense, less magnetic, and lower-velocity strata to the north. Paleoseismologic studies indicate several large, middle to late Holocene earthquakes occurred on the Seattle fault [e.g., *Bucknam et al.*, 1992; *Sherrod et al.*, 2000; *Nelson et al.*, 2002, 2003a, 2003b]. Complex gravity and magnetic gradients also mark the southern end of the Seattle uplift, along the boundary with the Tacoma basin [*Pratt et al.*, 1997; *Brocher et al.*, 2001]. *Gower et al.* [1985] suggested either a fault or a monoclinal fold caused these anomalies but provided no documentation. On the basis of seismic reflection data, *Pratt et al.* [1997] proposed that this structural zone is a monoclinal fold that formed above a thrust fault that underlies the Seattle uplift. In contrast, seismic tomographic models led *Brocher et al.* [2001] to propose that the boundary between the Seattle uplift and the Tacoma basin is a steep, north dipping reverse fault, which they refer to as the "Tacoma fault." Paleoseismological studies have documented late Holocene uplift and subsidence along this boundary [*Bucknam et al.*, 1992; *Sherrod et al.*, 2002, 2003] and accurate characterization of its geometry and history are essential to regional seismic hazard assessment.

[6] This paper presents a summary of seismic reflection and relevant geologic and geophysical data across the boundary between the Seattle uplift and Tacoma basin, and concludes that parts of both of the seemingly contradictory structural models outlined above [*Pratt et al.*, 1997; *Brocher et al.*, 2001] are correct. Our data show that the northwestern margin of the Tacoma basin is a north dipping thrust fault, the Tacoma fault, and that the northeastern basin margin is defined by a south dipping monocline, which we here refer to as the Rosedale monocline. Furthermore, we suggest that the hanging wall of the Tacoma fault overlies the northwestern extent of the Rosedale monocline. Our investigations indicate that shortening along this structural zone may be as much as 2–3 mm/yr, accommodating a significant portion of the 4–6 mm/yr of shortening suggested by GPS-based deformation models for the Puget Lowland [*Khazaradze et al.*, 1999; *Miller et al.*, 2001; *Mazotti et al.*, 2002].

2. Geophysical and Geologic Mapping

[7] Our analysis of the tectonics of the south flank of the Seattle uplift relies in part on gravity, aeromagnetic, and seismic reflection surveys and geologic mapping, described below.

2.1. Gravity

[8] The gravity gradient that occurs along the boundary between the Seattle uplift and the Tacoma basin (Figure 2a) [*Danes et al.*, 1965; *Finn et al.*, 1991] is here termed the "Gig Harbor gravity gradient" after the Puget Sound community that lies along its trace (Figure 2a). This gravity gradient has a notably arcuate shape, characterized by a west trending western segment and a northwest trending eastern segment. The gravity gradients along the western and eastern segments are about 6 mgals/km and 2–3 mgals/km, respectively. *Pratt et al.* [1997] and *Hagstrum et al.* [2002] modeled the eastern portion of the gradient as a southwest dipping monocline in which dense basalt of the Eocene Crescent Formation rises to the northeast.

[9] Gravity mapping also shows a steep, north trending gradient along the west flank of the Seattle uplift. The small (~12 km wide), wedge-shaped gravity low that occurs west of the Seattle uplift is herein referred to as the "Dewatto basin" after a local community.

2.2. Aeromagnetics

[10] The west trending aeromagnetic gradient on the northwest margin of the Tacoma basin is here referred to as the "Allyn aeromagnetic gradient," after a small town that occurs along northern Case Inlet where the gradient is steepest, about 250 nT/km (Figure 2b). The Allyn gradient coincides with the west trending western segment of the Gig Harbor gravity gradient but, unlike the gravity gradient, does not bend to the southeast toward Tacoma. Depending on how it is defined, the magnetic gradient could either end to the east near northern Carr Inlet, or it could continue its easterly trace to the southern margin of a magnetic high on southern Vashon Island. The source of the Allyn gradient is inferred to be shallow basaltic rocks of the Eocene Crescent Formation (see below). Aeromagnetic mapping also reveals a steep gradient on the western margin of the Seattle uplift adjacent to the Dewatto basin aeromagnetic low. The Dewatto basin appears to be separated on the south from the Tacoma basin by low-amplitude gravity and magnetic (Figure 2b) highs.

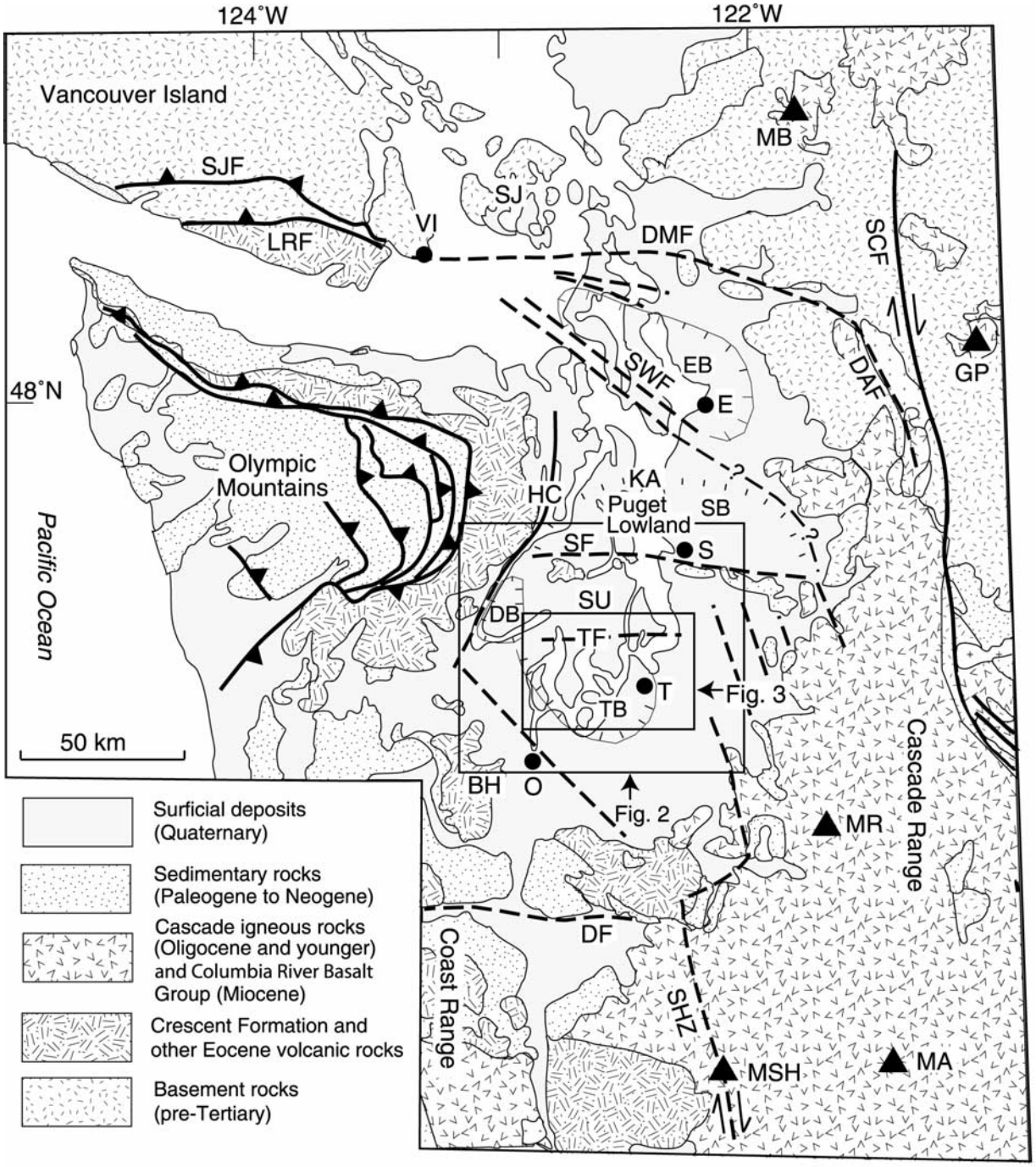

Figure 1. Schematic geologic map of northwestern Washington showing the Puget Lowland and flanking Cascade Mountains, Coast Range, and Olympic Mountains. Abbreviations for cities are as follows: O, Olympia; S, Seattle; T, Tacoma; VI, Victoria. Abbreviations for faults (heavy lines), modern Cascade volcanoes (triangles) and other geologic features are as follows: BH, Black Hills; DAF, Darrington fault; DB, Dewatto basin; DF, Doty fault; DMF, Devils Mountain fault: E, Everett; EB, Everett Basin; GP, Glacier Peak; HC, Hood Canal; KA, Kingston arch; LRF, Leech River fault; MA, Mount Adams; MB, Mount Baker; MR, Mount Rainier; MSH, Mount Saint Helens; SB, Seattle basin; SCF, Straight Creek fault; SF, Seattle fault; SU, Seattle uplift; SHZ, Saint Helens zone; SJ, San Juan Islands; SJF, San Juan fault; SWF, southern Whidbey Island fault; TB, Tacoma basin; TF, Tacoma fault. Boxes show areas of Figures 2 and 3. Geology from maps and compilations of *Tabor and Cady* [1978], *Washington Public Power Supply System* [1981], *Gower et al.* [1985], *Walsh et al.* [1987], *Whetten et al.* [1988], *Yount and Gower* [1991], and *Tabor et al.* [1993].

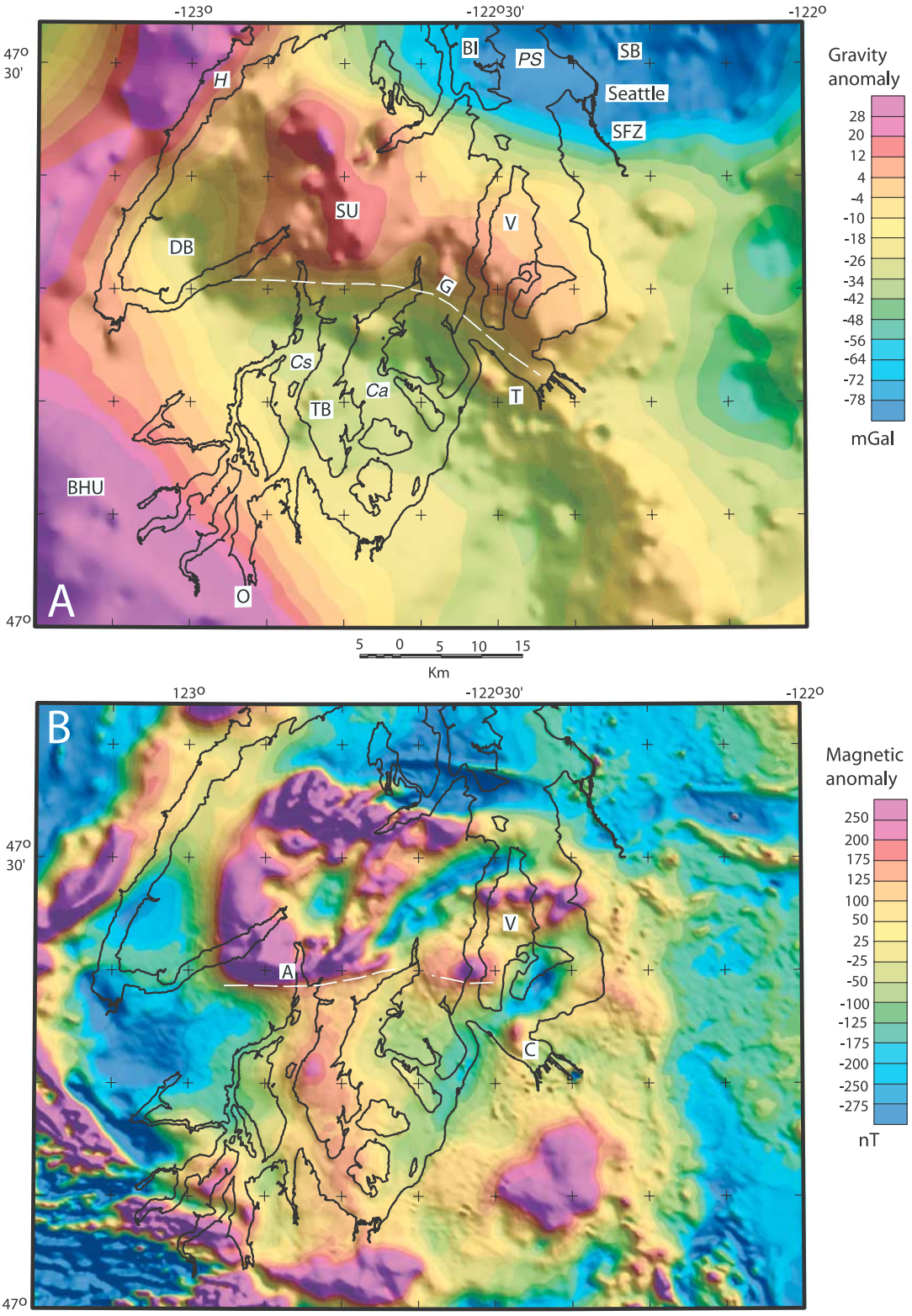

Figure 2. (a) Isostatic residual gravity anomaly map [from *Finn et al.*, 1991], and (b) aeromagnetic anomaly map [from *Blakely et al.*, 1999] of the central Puget Lowland, Washington. Dashed white lines show locations of Gig Harbor gravity gradient (G) and Allyn aeromagnetic gradient (A). BI, Bainbridge Island; BHU, Black Hills uplift; C, Commencement Bay; Ca, Carr Inlet; Cs, Case Inlet; DB, Dewatto basin; H, Hood Canal; O, Olympia; PS, Puget Sound; SFZ, Seattle fault zone; SU, Seattle uplift; T, Tacoma; TB, Tacoma basin; V, Vashon Island.

[11] In the Figure 2 map area, aeromagnetic and gravity highs generally correlate with local uplifts and sedimentary basins. There are, however, places where aeromagnetic highs correspond to gravity lows, such as in the southern Tacoma basin (47°8′, 122°20′). In that the gravity and nearby seismic reflection data [*Pratt et al.*, 1997] (also see below) indicate the Crescent Formation is buried several kilometers in this area, the aeromagnetic high must indicate relatively magnetic post-Crescent strata, perhaps Eocene or Oligocene volcanic or volcaniclastic rocks. There are also a few places where aeromagnetic lows correspond to areas where other geophysical data suggest the Crescent Formation is within a few kilometers of the surface, such as in the central Seattle uplift north of Carr Inlet, and along the southeast flank of Maury Island (Figures 3 and 4). *Hagstrum et al.* [2002] inferred that the aeromagnetic lows in these areas were caused by reversely magnetized Crescent Formation.

2.3. Seismic Reflection

[12] Our investigation of active structures in the southern Puget Sound region relies on a network of multichannel, high-resolution seismic reflection data collected in 1997 by the U.S. Geological Survey (Figure 3a). For this survey, the seismic source was a two-chambered, 1147 cm^3 airgun fired at 20 m intervals, and data were digitally recorded for 2 s with a 24-channel (10-m group interval; 240-m active length) streamer. Resulting common midpoint (CMP) stacked data are 6-fold and have a 5-m CMP spacing. Profiles were located using GPS satellite navigation with an accuracy of ±10–20 m. These data were deconvolved and filtered before and after stacking, then time-migrated using a smoothed velocity function. Data are typically of highest quality in the upper approximately 0.5–0.7 s and degrade significantly with greater depth. Deconvolution was only partly effective in suppressing water-bottom multiples, especially in shallow water.

[13] We examined several seismic reflection profiles that penetrated deeper into the section (Figure 3b) with lower vertical resolution. These included two SHIPS (Seismic Hazards in Puget Sound) project profiles (Figure 3b [*Fisher et al.*, 1999) collected in 1998 using a 79.3-L (4838 cubic inches) airgun array and a 2.4-km-long, 96-channel (25-m group interval) streamer. Stacked data are 24-fold and have 12.5 m CMP spacing. These data were stacked, deconvolved and filtered, and then time-migrated using a smoothed velocity function.

[14] Finally, we examined several industry seismic reflection profiles (3 to 5 s records) that were collected with airgun sources of various sizes in the late 1960s and early 1970s when the region was considered a petroleum exploration frontier. Although we have digital records for some of these profiles, much of the data was made available to us only as variably degraded paper records. For the two Mobil profiles that are included in this report, data were recorded for 5 s on a 24-channel, 1402-m-long streamer. Stacked data are 24 fold and have a 30.5 m CMP spacing. Regional coverage by these deeper, lower-frequency, lower-resolution profiles was less than that of the high-resolution survey (Figure 3).

2.4. Geologic Mapping

[15] Local geologic mapping was conducted on all of the shorelines of south central Puget Sound in the vicinity of the Gig Harbor gravity gradient, Allyn aeromagnetic gradient, Tacoma fault, and Rosedale monocline (Figures 2 and 4). The purpose of this mapping is to further confirm and clarify the style, geometry, and rates of Quaternary deformation with field observations. Given the Quaternary glacial history of the region (see below), differentiating between tectonic and glaciotectonic deformation [e.g., *Van Der Meer*, 1987; *Croot*, 1988; *Aber et al.*, 1989; *Aber*, 1993], each of which can produce outcrop scale faults and folds, is obviously important and can be difficult. In this study and in our previous similar investigations in the Puget Lowland [e.g., *Johnson et al.*, 1996, 1999, 2001], we have learned that deformed Quaternary strata in the Puget Lowland are generally concentrated along projections of faults imaged on nearby offshore seismic reflection profiles and have a structural style and geometry consistent with that of the larger-scale fault or fold imaged on the seismic reflection data. Where there is not this coincidence of seismic reflection and outcrop data, or where structural styles are inconsistent in the two data sets, as in some cases described below, glaciotectonic deformation is considered likely.

3. Stratigraphy and Seismic Stratigraphy

[16] Four stratigraphic units underlie the study area and are imaged on marine seismic reflection data [*Johnson et al.*, 1994, 1999, 2001; *Pratt et al.*, 1997]. These units include Eocene Crescent Formation volcanic rocks, Eocene and younger sedimentary rocks, uppermost Pliocene (?) to Pleistocene strata, and uppermost Pleistocene to Holocene postglacial strata. The older two units occur only in the subsurface of much of this portion of the Puget Lowland (Figure 4) and are not distinguished on the seismic reflection profiles included herein. Surface exposures in the region consist almost entirely of Pleistocene glacial and interglacial deposits, also widespread at the seafloor and in the shallow subsurface offshore. The youngest unit occurs primarily as the fill of alluvial valleys onshore and of glacial erosional channels offshore. For this report, the older two units are distinguished from the younger two Quaternary units on seismic reflection profiles based on stratigraphic position and seismic stratigraphic facies [e.g., *Sangree and Widmier*, 1977; *Stoker et al.*, 1997].

3.1. Crescent Formation

[17] Predominantly marine basaltic rocks of the Eocene Crescent Formation form the basement below the southern Puget Lowland. These rocks tend to be dense and magnetic, and are considered to be responsible for the gravity and magnetic highs measured over the Seattle uplift [*Blakely et al.*, 2002; *Hagstrum et al.*, 2002] (Figures 1 and 2). The Crescent Formation crops out in the northern part of the Seattle uplift [*Yount and Gower*, 1991; *Haeussler and*

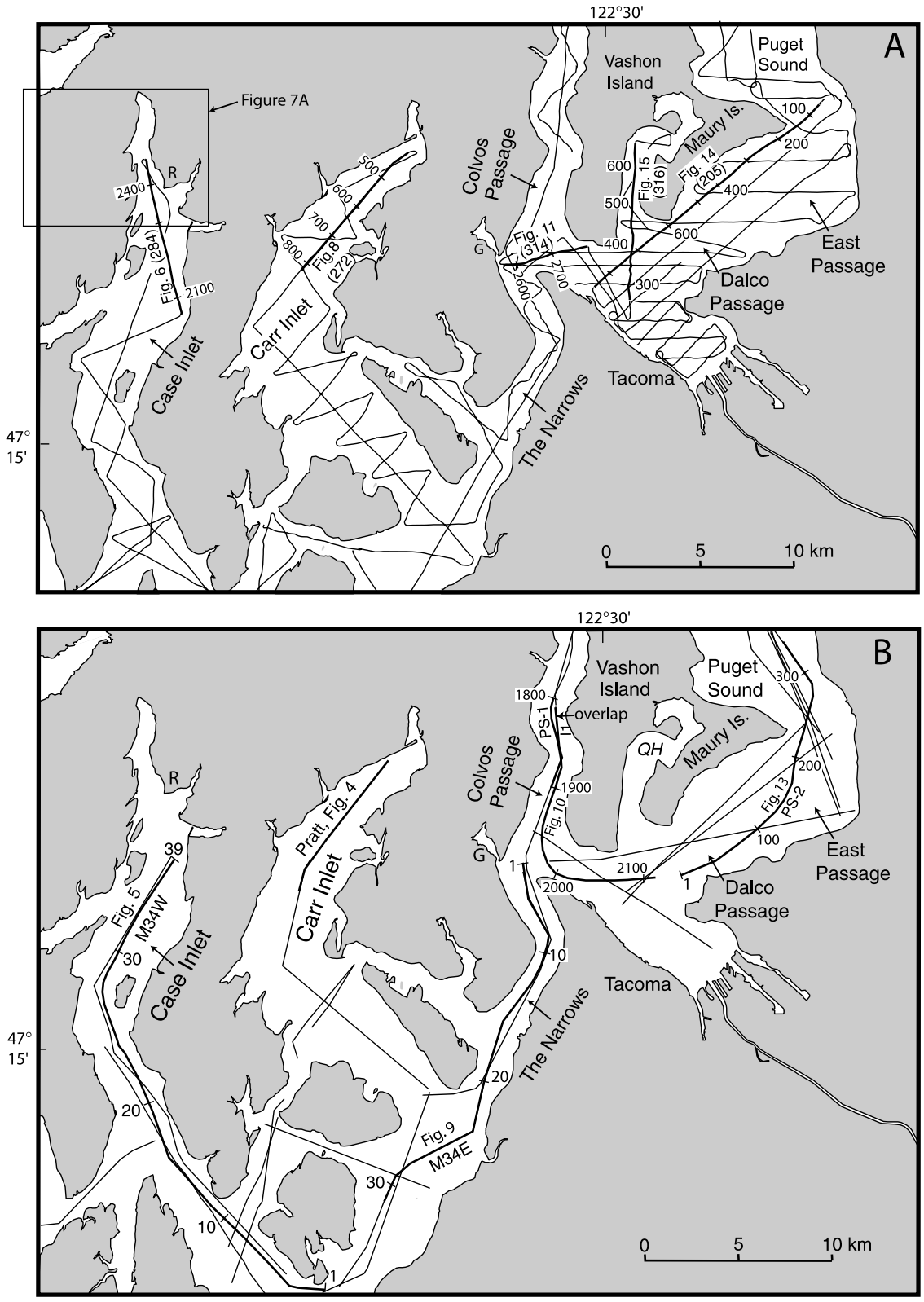

Figure 3. (a) Map showing tracklines of 1997 U.S. Geological Survey high-resolution seismic reflection survey, highlighting profiles displayed in this report. Labeled ticks show shot points. Box shows area of Figure 7. (b) Map showing locations of lower-frequency industry seismic reflection profiles available to this investigation, and the location of SHIPS survey [*Fisher et al.*, 1999] track lines. Labeled ticks show shot and location points. G, Gig Harbor; QH, Quartermaster Harbor; R, Rocky Point.

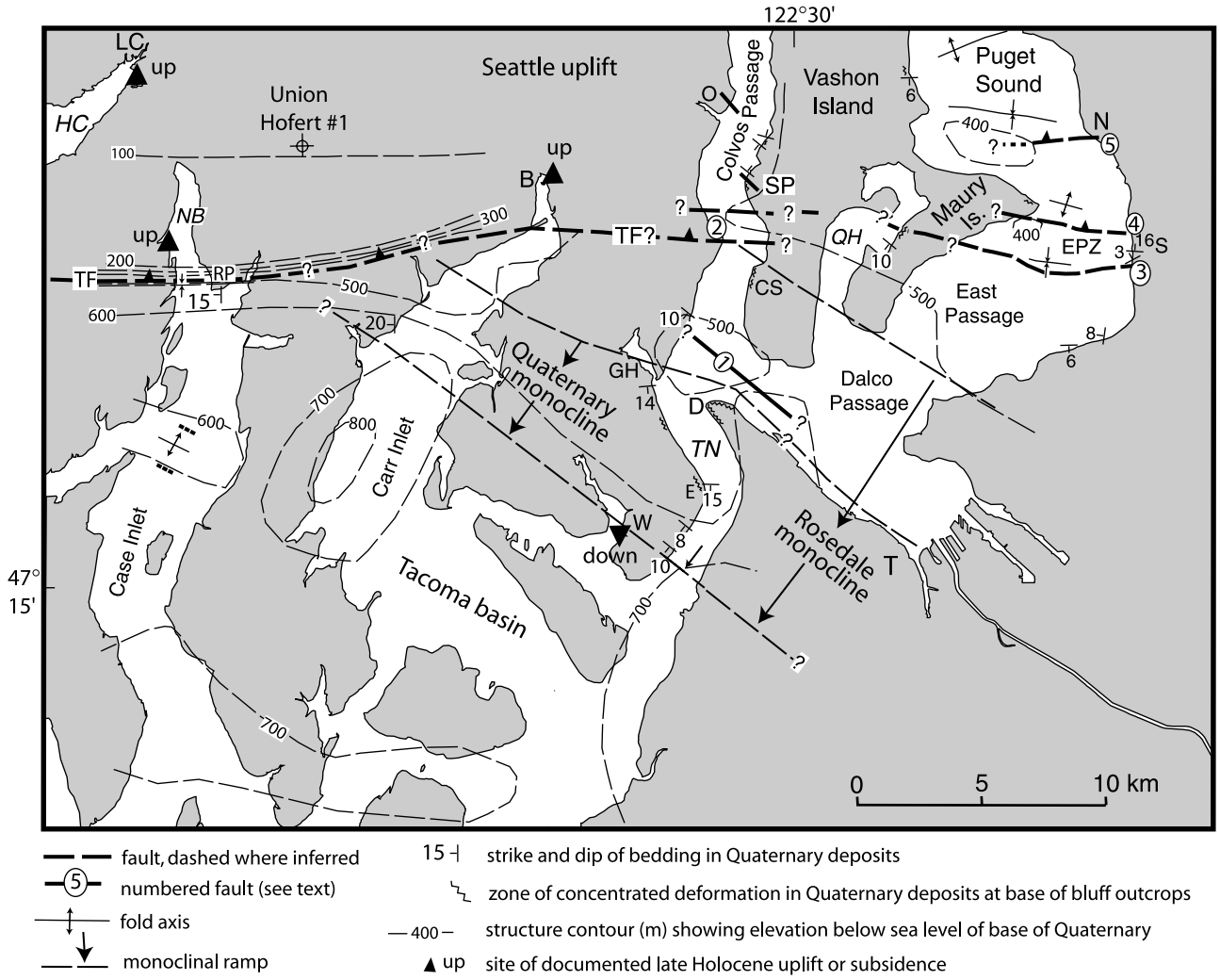

Figure 4. Map showing selected geologic features and structural interpretation of south central Puget Lowland (Figure 1). The entire area is underlain by Quaternary deposits. Dips plotted on map are all from discontinuous exposures of Pleistocene strata at the base of coastal bluffs; exposures with dipping strata are commonly separated by zones of flatlying Quaternary strata and are generally unconformably overlain by flatlying strata higher in the bluffs. Dips in Quaternary strata are generally minor (<5°) unless shown. B, Burley; CS, Camp Sealth; D, Point Defiance; E, Point Evans; EPZ, East Passage zone; GH, Gig Harbor; HC, Hood Canal; LC, Lynch Cove; N, Normandy Beach Park; NB, North Bay; O, Olalla; QH, Quartermaster Harbor, RP, Rocky Point; S, Saltwater State Park; SP, Sandford Point, T, Tacoma; TF, Tacoma fault; TN, The Narrows; W, Wollochet. Triangles show areas of ∼A.D. 900 uplift and subsidence [*Bucknam et al.*, 1992; *Sherrod et al.*, 2002, 2003].

Clark, 2000], in a rim surrounding the core of the Olympic Mountains [*Tabor and Cady*, 1978], and on the south flank of the Tacoma basin in the Black Hills [*Walsh et al.*, 1987] (Figure 1). The Crescent Formation was also penetrated at a depth of 213 m in the Union Hofert 1 well, a few kilometers north of the Gig Harbor gravity gradient and Allyn magnetic gradient between Carr and Case Inlets (Figure 4) [*Sceva*, 1957]. The upper part of the Crescent Formation consists of interbedded basalt and sedimentary rocks [*Babcock et al.*, 1992]. Industry seismic reflection data commonly image as much as 1–2 km (>1 s two-way travel time (TWTT)) of the upper Crescent Formation) [*Johnson et al.*, 1994, 1999, 2001; *Pratt et al.*, 1997], which is represented by variable to high amplitude, discontinuous, subparallel to low-angle reflections with common intraformational onlap surfaces. Potential-field, tomography, and refraction data indicate the Crescent Formation and its igneous basement may be 25–30 km thick in western Washington [*Finn*, 1990; *Lees and Crosson*, 1990; *Tréhu et al.*, 1994].

3.2. Tertiary Sedimentary Rocks

[18] Tertiary sedimentary rock units are inferred to overlie the Crescent Formation in the subsurface of the

Tacoma basin and are at least locally present above the Crescent beneath the Seattle uplift. These rocks probably include correlatives of the Eocene nonmarine to marginal marine strata of the Puget Group which crop out to the east in the Cascade Range foothills, and the Oligocene Blakeley Formation, which crops out on the north flank of the Seattle uplift [*Yount and Gower*, 1991; *Johnson et al.*, 1994]. On industry seismic reflection profiles, Tertiary sedimentary rocks are characterized by relatively continuous, moderate- to high-amplitude, parallel to subparallel reflections. In the Puget Lowland, the contact between Tertiary sedimentary rocks and the underlying Crescent Formation interpreted on seismic reflection profiles is generally conformable or characterized by a low-angle unconformity [*Johnson et al.*, 1994, 1996, 1999, 2001; *Pratt et al.*, 1997].

3.3. Uppermost Pliocene(?) to Pleistocene Strata

3.3.1. Onshore Stratigraphy

[19] Uppermost Pliocene(?) to Pleistocene deposits of the Puget Lowland comprise a stratigraphically complex unit of glacial, transitional, and interglacial deposits that are locally as thick as 1100 m [*Yount et al.*, 1985; *Jones*, 1996]. The composite section contains six or more glacial drifts [*Blunt et al.*, 1987; *Easterbrook*, 1994]. Glacial drift typically consists of till and outwash; transitional facies comprise fluvial and glaciolacustrine deposits; interglacial deposits are typically fluvial and deltaic, including peat. Mapping these units has proven difficult for several reasons. (1) Similar lithologies and lithofacies can belong to different units with different ages. (2) There is considerable erosional relief between units, and strata of one age can occur at elevations with a range of as much as 230 m [*Troost*, 1999, 2002]. (3) Only strata of the youngest glacial advance (Vashon) and the youngest part of the preceding Olympia interglacial period can be confidently dated with radiocarbon techniques. There are only a few dates or constraints on the ages of older Quaternary units [*Mahan et al.*, 2000; *Hagstrum et al.*, 2002]. As a result, geologic maps in the region commonly group strata that is inferred to be older than the pre-Olympia interglacial interval [e.g., *Booth*, 1991]. (4) All six glacial drift units may be exposed in the Tacoma region [*Troost*, 1999]. In other areas of the Puget Lowland such as Whidbey Island, geologic mapping and Pleistocene stratigraphic investigations are more straightforward because fewer stratigraphic units are present at the surface and in the shallow subsurface [*Easterbrook*, 1968; *Johnson et al.*, 2001].

[20] For this investigation, we attempted to constrain possible Quaternary faulting or folding on southern Vashon and Maury Islands using Quaternary stratigraphic cross sections based on water-well logs, similar to the effort of *Johnson et al.* [2001] for the Devils Mountain fault zone on northern Whidbey Island. We plotted the lithologies of more than 100 wells (depths of 40 to 200 m) but were unable to confidently correlate subsurface stratigraphy across the area and to define stratigraphic markers to constrain deformation. This lack of stratigraphic continuity is mainly attributable to repeated pulses of large-scale glacial and glaciofluvial scour and fill, but could also partly reflect local tectonic disruption.

3.3.2. Offshore Stratigraphy

[21] Two seismic units occur above the Tertiary section in the Tacoma region. On both industry and higher resolution seismic reflection data, the lower of these two units consists of seismic facies typical of glacial deposits [*Davies et al.*, 1997]. Characteristics include discontinuous, variable-amplitude, parallel, divergent, and hummocky reflections, with common internal truncation, onlap, and offlap of reflections. On the basis of this seismic character and on stratigraphic position, this lower unit is inferred to comprise uppermost Pliocene(?) to Pleistocene deposits. Regional physiography suggests that the presently submerged regions of the Puget Sound area formed as subglacial erosional channels [*Booth*, 1994] that were partly filled in with fluvial and lacustrine sediment during ice retreat. Thus, much of the Quaternary fill imaged by marine seismic reflection data in the Tacoma region is of recessional origin. We did not recognize any internal sequences within the inferred uppermost Pliocene(?) to Pleistocene section that could be traced across the region and might correlate with the multiple glacial and nonglacial intervals. We attribute this lack of internal stratigraphy to repeated irregular and large-scale glacial erosion (during ice advance) and deposition (during ice retreat). On industry seismic reflection data, the Tertiary-Quaternary contact is typically imaged as a moderate- to high-amplitude, fairly continuous reflection separating higher amplitude, more continuous, commonly parallel reflections (Tertiary sedimentary rocks and Crescent Formation) from lower-amplitude, discontinuous, hummocky or irregular reflections (Quaternary strata). On the Seattle uplift, the Tertiary rocks are locally folded and the contact is locally an angular unconformity. This angular unconformity passes laterally into a disconformity to the south in the Tacoma basin.

3.3.3. Identification and Age of the Base of the Uppermost Pliocene(?) to Pleistocene Section

[22] As outlined above, the base of the inferred uppermost Pliocene(?) to Pleistocene seismic unit is typically more distinct on conventional industry seismic reflection data, where it can commonly be recognized on the basis of contrasts in seismic facies [*Johnson et al.*, 1994, 1996, 1999, 2001] and local angular unconformities. On high-resolution seismic reflection profiles (Figure 3a), the contrast in seismic facies between Tertiary and mainly Quaternary strata ranges from quite distinct to irresolvable. In our interpretation of these profiles, the location of the contact is generally based on projection from nearby conventional industry profiles or on the basis of locally distinct unconformities and onlapping surfaces. Once the contact at the base of the mainly Quaternary section is identified at one or more locations on individual high-resolution profiles, it can generally be traced across the profile based on reflection continuity. Complete coverage through the central Puget Sound waterways is thus accomplished by iteratively combining the industry and high-resolution data. Figure 4 includes a contour map of depth to the base of the Quaternary section based on these data and a single bore-

hole (Union Hofert 1). Depths estimated from the seismic reflection data assume velocities of 1800 m/s for Quaternary strata [*Johnson et al.*, 1994, 1996, 2001; *Pratt et al.*, 1997; *Brocher and Ruebel*, 1998].

[23] Knowing the age of the base of the uppermost Pliocene(?) to Pleistocene section in offshore data is important because it provides a potential time marker for estimating rates of Quaternary deformation. Determining this age is, however, problematic. No boreholes have penetrated the offshore section, and multiple pulses of deep subglacial scour and subsequent filling in offshore areas suggest that the age of the basal surface may vary locally and that correlation with adjacent dated units on land is untenable. For this investigation, we infer that this surface has a maximum age of ~2 Ma, coinciding with the age of the first glaciation for which there is evidence in the Puget Lowland [*Easterbrook*, 1994], slightly older than the Pliocene-Pleistocene boundary [*Gradstein and Ogg*, 1996]. Because of repeated deep glacial erosion, however, we think it probable that the oldest deposits in this unit imaged on many seismic reflection profiles are much younger than 2 Ma.

3.4. Uppermost Pleistocene and Holocene (Postglacial) Strata

[24] Variable-amplitude, parallel, and generally continuous reflections that fill local basins bounded by Pleistocene bathymetric highs characterize the uppermost unit on our seismic reflection profiles. These sediments are inferred to be mainly clay, silt, and sand derived from the Puyallup and Nisqually rivers, several smaller rivers and creeks, and erosion of Pleistocene deposits from unstable coastal bluffs. These sediments are inferred to be significantly reworked and redistributed by the strong tidal currents that characterize Puget Sound waterways.

4. Local Geology and Geophysics

[25] The geology and geophysics of four discrete areas along the southern margin of the Seattle uplift are described below, followed by brief discussions that provide local context and interpretation. Following descriptions of these four areas, the data are synthesized and interpreted at the regional scale.

4.1. Case Inlet

4.1.1. Mobil Line 34W (Figure 5)

[26] Mobil seismic reflection profile 34W extends northward through Case Inlet (Figure 3), ending about 3.1 km south of Rocky Point. The profile crosses much of the western Tacoma basin and is characterized by relatively flat (1° > mean dip), moderate- to high-frequency, moderate-amplitude reflections along most of its length. Basinal strata are locally folded into a small gentle anticline near the north end of profile. Dips on the fold limbs are as steep as 10°–11°, and appear to extend upward into the lower part of the Quaternary section. Quaternary and total structural relief on this fold are about 75 to 100 m and 175 to 225 m, respectively. The north limb of the fold is truncated below about 1.5 to 2.0 s (TWTT) by a steep (~75°) south dipping reverse fault; the south limb of the fold appears to be cut by a north dipping (~50°) fault below about 2.5 s (TWTT). This fault-bounded fold resembles positive flower structures, as described by *Harding* [1985].

4.1.2. U.S. Geological Survey Line 284 (Figures 6 and 7b)

[27] U.S. Geological Survey (USGS) seismic reflection line 284 passes through northern Case Inlet (Figure 3), extending about 1.4 km north of Rocky Point. The south end of the profile lies about 2.3 km east of Mobil 34W; the two profiles cross at the north end of Mobil 34W (Figure 3). Reflections are very gently folded at the southern end of line 284, indicating that relief on the gentle anticline imaged on Mobil 34A diminishes to the east.

[28] Tertiary and Quaternary strata at the north end of the profile (~shot 2425; about 400 m north of Rocky Point) are folded above a steep, north dipping, blind reverse fault, best viewed on the 1:1 image of Figure 7b. Although not obvious, the fault appears to extend to within about 500–600 m (~0.6 s TWTT) of the surface, truncating and juxtaposing reflectors in Tertiary strata with contrasting amplitude and frequency. South dipping (~35°) reflections in inferred Tertiary strata above the fault form a ~360-m-wide, constant-width, kink band. Overlying Quaternary strata form a southward narrowing growth triangle [e.g., *Suppe and Medwedeff*, 1990; *Suppe et al.*, 1992; *Shaw and Suppe*, 1994]. The precise location of the upper boundary of this triangle, the growth inactive axial surface, is defined by the change from subhorizontal to south dipping beds and is partially obscured by water-bottom multiples.

4.1.3. Relevant Geologic Data

[29] There are few exposures in the heavily vegetated, low-relief coastal regions bounding northern Case Inlet. Sparse outcrops of glacial diamict and fluvial deposits along the projection of the fault on the east side of North Bay are cut by small faults and fractures of uncertain (e.g., tectonic or glaciotectonic) origin. Interbedded diamict and sand and gravel exposed for about 100 m along the south facing coastal bluffs east of Rocky Point dip as much as 15° west (Figure 4).

[30] The upper hinge of the kink band imaged on USGS seismic reflection line 284 (Figure 6) lies on strike with and 2 km east of the eastern expression of a discontinuous, ~3.5-km-long, 1- to 3-m-high, north-side-up, west trending scarp detected by airborne laser swath mapping (Figure 7). Two trenches on this scarp revealed shearing, folding, and minor faulting in undated till [*Sherrod et al.*, 2003; A. R. Nelson, personal communication, 2003]. The age of deformation is considered postglacial (<15 ka) because the Puget Sound landscape is widely considered latest Pleistocene in age, relict from the most recent glaciation [e.g., *Booth*, 1994]. All known fault scarps in the Puget Lowland that have been dated are of postlgacial age [e.g., *Wilson et al.*, 1979; *Nelson et al.*, 2002, 2003a, 2003b; *Johnson et al.*, 2003; *Sherrod et al.*, 2003]. Older fault scarps and other landforms are assumed to have been eroded, buried, or otherwise modified by glacial processes.

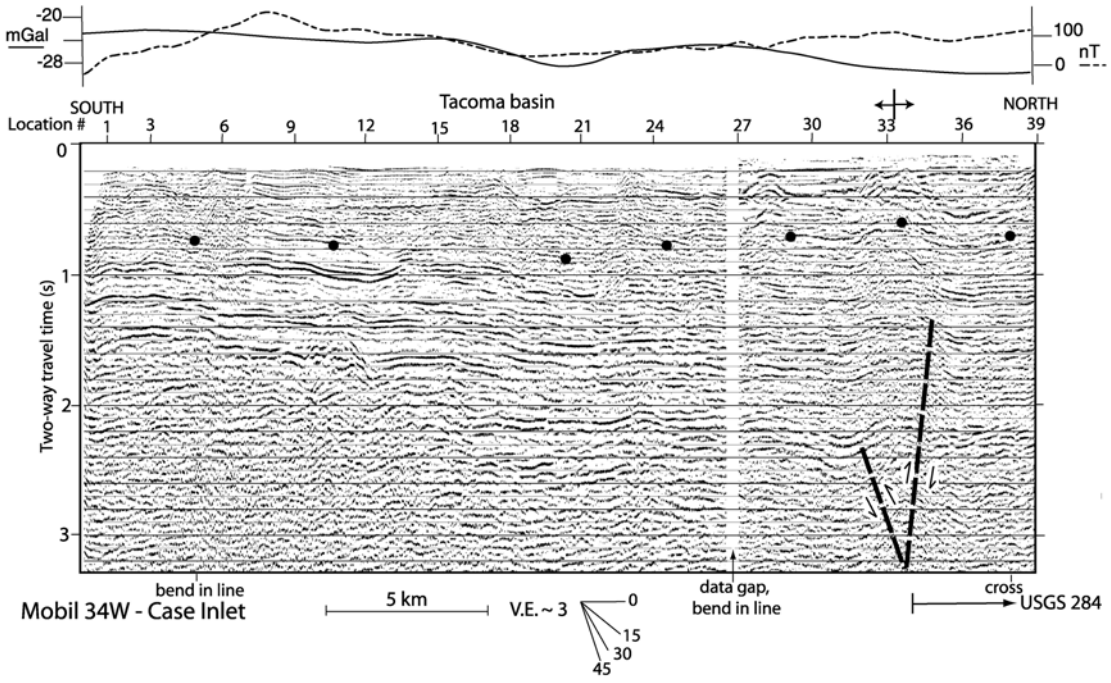

Figure 5. Mobil 34W seismic reflection profile, gravity profile, and aeromagnetic profile, Case Inlet (Figure 3b). Solid dots show the inferred base of the Quaternary section and heavy dashed lines show inferred faults. Gravity profile (solid line) and aeromagnetic profile (dashed line) extracted from Figure 2.

[31] Paleoseismologic investigations based on marsh stratigraphy also indicate uplift (from 1.5 m to as much as 4 m) in the past ~3000 years in North Bay (Figure 4) [*Sherrod et al.*, 2002] north of the inferred north dipping fault. This uplift is consistent with that noted by *Bucknam et al.* [1992] from Lynch Cove (>2 m) and Burley (Figure 4), sites that also lie north of the Gig Harbor gravity gradient and Allyn magnetic gradient (Figure 2). This uplift significantly postdates postglacial rebound, which was largely completed by about 10–12 ka [e.g., *Dethier et al.*, 1995).

[32] The contours on the base of the Quaternary in this area are based on the interpretation in Figure 6 and on the Union Hofert 1 borehole, the only known well in this area that penetrated through the Quaternary section to bedrock.

4.1.4. Discussion

[33] The blind fault imaged on USGS 284 (Figure 6) coincides with the Gig Harbor gravity gradient and the Allyn aeromagnetic gradient (Figure 2), and a steep velocity gradient [*Brocher et al.*, 2001] representing the boundary between the Seattle uplift and the Tacoma basin. We follow *Brocher et al.* [2001] in designating this fault the "Tacoma fault." Using methods described by *Schneider et al.* [1996] for assessing folding above blind faults, Quaternary shortening across the kink band (Figure 6) is about 120 m, the thickness of Quaternary growth strata is about 360 m, fault dip is approximately 71°, and the amount of Quaternary fault slip needed to generate the growth fold is about 380 m.

[34] The tomography cross section *of Brocher et al.* [2001, Plate 3] at this longitude suggests the top of the Crescent Formation south of the Tacoma fault is at a depth of 6 to 7 km, yielding an estimate of the total amount of structural relief across the zone. However, the northward thickening of the Tacoma basin approaching the Tacoma fault predicted by the tomographic model is not apparent from existing seismic reflection data (Figure 5). If the basin fill does thicken northward, it must occur below the level of the stratigraphy imaged on Mobil 34W (~4–5 km, Figure 5).

[35] The onset of deformation along the Tacoma fault correlates with the pregrowth-growth boundary within the kink band [*Suppe et al.*, 1992], which occurs at the top of the Tertiary section (Figure 6). Because the Tertiary-Quaternary contact is an inferred unconformity (see above) and the age of the uppermost Tertiary strata in this area is not known, the timing of the onset of deformation cannot be precisely determined. The lack of significant thickening within Tacoma basin strata in younger Tertiary and Quaternary strata approaching the Tacoma fault (Figures 5 and 6), which would be predicted by contractional faulting, folding, and basin-margin crustal loading, is consistent with the onset of deformation being relatively recent (i.e., Quaternary). The presence of an obvious scarp above the upper fold axis in the kink band (Figure 7) indicates Holocene activity on this structure.

4.2. Carr Inlet

4.2.1. Industry Seismic Reflection Profile

[36] *Pratt et al.* [1997, Figure 4] show an industry seismic reflection profile that extends northward through Carr Inlet (Figure 3). At its southern end, the profile images flat (dip < 1°) reflectors in the Tacoma basin. These basinal reflectors are warped upward at the north end of the profile into a south

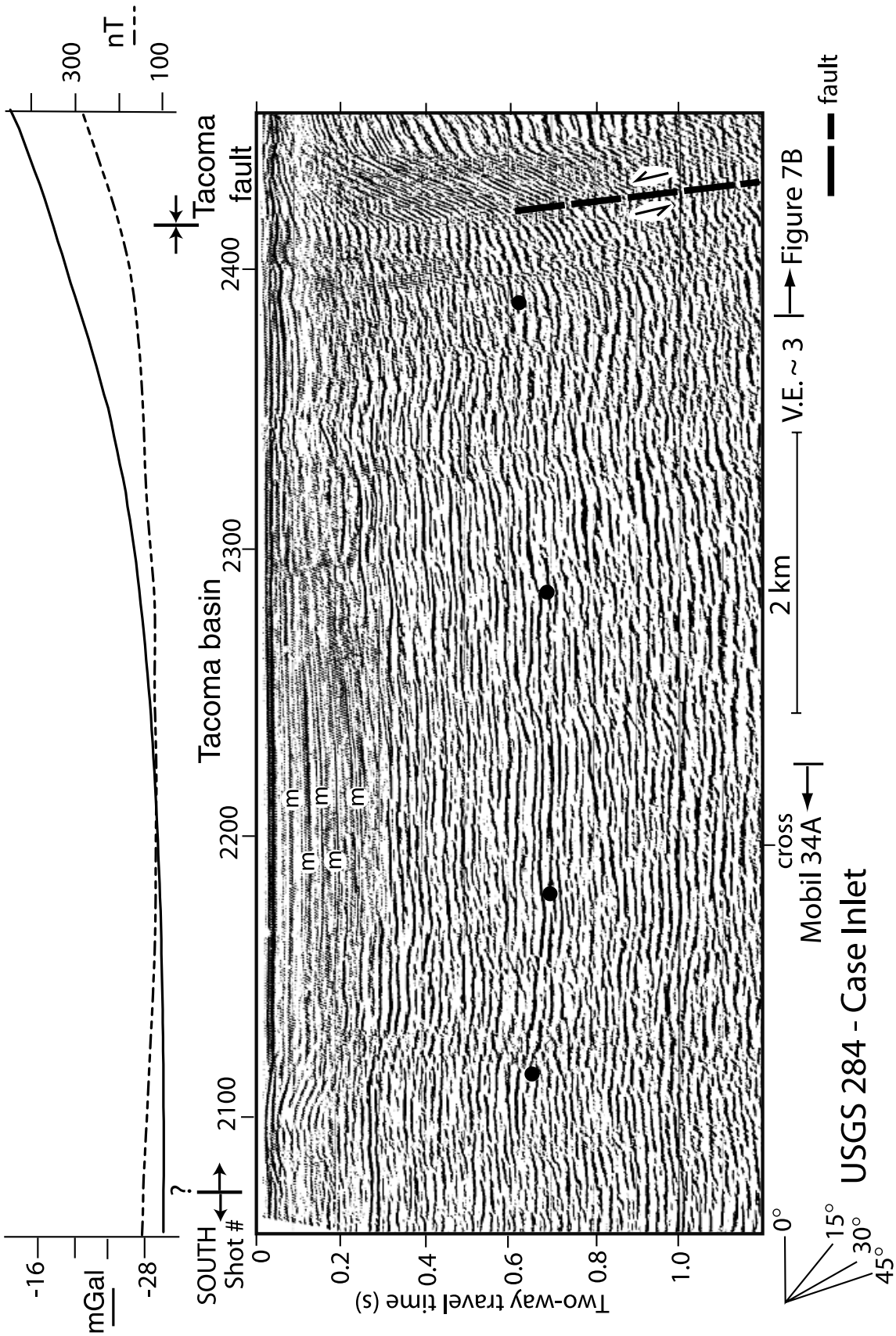

Figure 6. U.S. Geological Survey seismic reflection profile 284, Case Inlet (Figure 3a). Solid dots show the inferred base of the Quaternary section and heavy dashed lines shows fault. The "m" shows water-bottom multiples. Gravity profile (solid line) and aeromagnetic profile (dashed line) extracted from Figure 2. Detailed 1:1 image of the fault zone at the northern part of the profile is shown in Figure 7b.

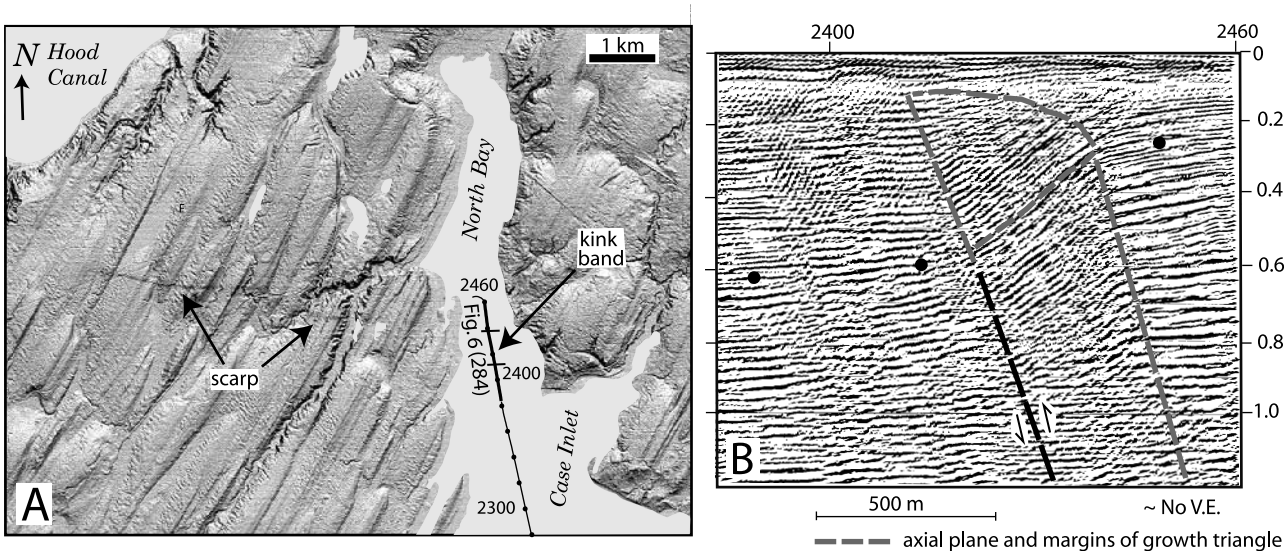

Figure 7. (a) Shot point map for USGS seismic reflection profile 284 (Figures 3 and 6) plotted on digital elevation model (DEM) derived from airborne laser swath mapping survey in the northern Case Inlet-North Bay area (Figure 3a). Note that a north-side-up, west trending scarp lies along strike with the upper hinge of the kink band imaged on line 284 (Figures 6 and 7b). Prominent north-northeast lineations on the landscape are of glacial origin. (b) Northern part of USGS profile 284 showing kink band.

dipping monocline, herein informally referred to as the "Rosedale monocline" after a local community that lies above the area of dipping strata. There is no obvious evidence of shallow (upper 4–5 km) faulting on the profile.

4.2.2. U.S. Geological Survey Line 272 (Figure 8)

[37] USGS Line 272 is nearly parallel to the industry profile shown by *Pratt et al.* [1997] (Figure 3), but extends 1050 m farther up Carr Inlet and provides significantly more detail in the upper 1 to 2 km. This profile also images flat reflectors in the Tacoma basin on the southwest that are warped upward at the northeast end of the profile into the southwest dipping Rosedale monocline. A prominent angular unconformity northeast of shot point 500 is inferred to be the base of the Quaternary section, associated with lowering of sea level and the occupation of Puget Sound by the first of several lobes of the continental ice sheet. South of shot point 540, this angular unconformity passes southward into a conformable surface within the monocline. Tertiary beds within the monocline dip approximately 16° to 19° south assuming velocities of 3000 to 3500 m/s [*Pratt et al.*, 1997]. Above the unconformity, strata of inferred Quaternary age have a similar dip in the middle of the monocline, but dip less steeply to the north and the south. The northern termination of the Rosedale monocline within Tertiary strata (subunconformity) lies north of U.S. Geological Survey Line 272; hence the width of the deeper, Tertiary portion of the monocline is more than the 7 km shown in Figure 8. In contrast, the panel of dipping Quaternary strata is completely imaged on Line 272 and has a width of approximately 4100 m. The width of the panel of south dipping Quaternary strata decreases upward, outlining a syndepositional growth triangle [*Suppe et al.*, 1992], for which the upper boundary (inactive axial surface) is defined by the change from subhorizontal to south dips. There is a gentle increase in gravity along USGS Line 272 (Figure 8), corresponding to the north rise of Tertiary rocks in the Rosedale monocline.

4.2.3. Relevant Geologic Data

[38] Quaternary glacial and interglacial strata are discontinuously exposed in coastal bluffs along northern Carr Inlet, adjacent to the monocline imaged in USGS Line 272. Strata in one exposure opposite the lowest part of the monocline dip 20° west-southwest (Figure 4), but there are no obvious dips in exposures farther northeast. *Bucknam et al.* [1992] presented evidence for coastal uplift at Burley at the northern end of Carr Inlet about 1100 years B.P., about 3 km north of the north end of Line 272 (Figure 4).

4.2.4. Discussion

[39] No fault comparable to the Tacoma fault imaged in northern Case Inlet (Figure 6) was imaged on seismic reflection data in northern Carr Inlet. If the Tacoma fault extends this far to the east, it must lie north of the Carr Inlet seismic reflection profiles (Figure 3) and south of the Burley uplift site [*Bucknam et al.*, 1992]. Alternatively, the fault must terminate below the depth (~5 km) of the industry seismic reflection profile shown by *Pratt et al.* [1997, Figure 4] with no obvious effect on overlying strata. The growth triangles imaged in Case Inlet and Carr Inlet are markedly different in both width (4100 m versus 360 m) and dip (~16°–19° versus 35°), suggesting different origins.

4.3. Narrows and Colvos Passage

4.3.1. Mobil 34E (Figure 9)

[40] Mobil seismic reflection profile 34E extends northward through The Narrows, ending approximately 700 m

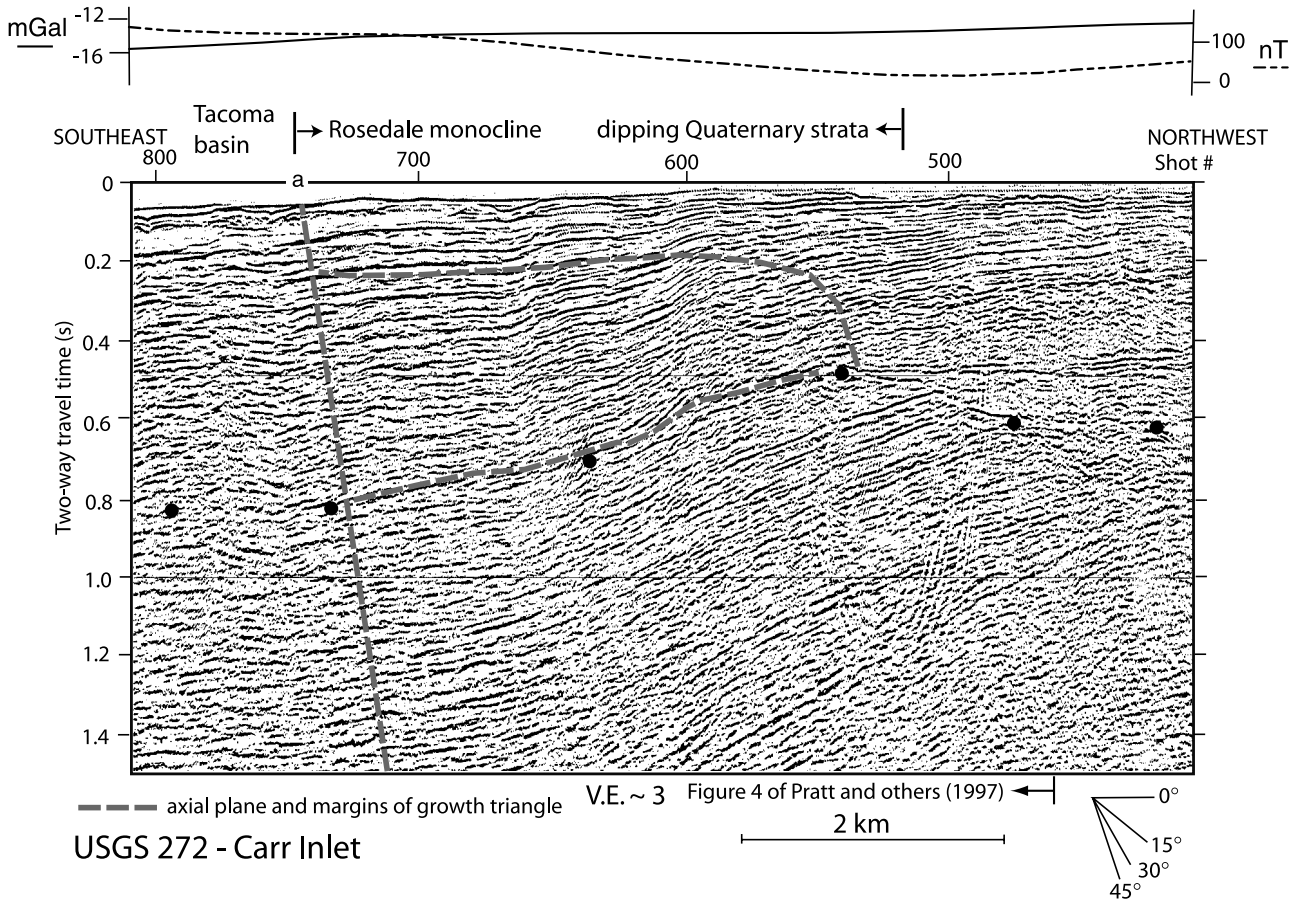

Figure 8. U.S. Geological Survey seismic reflection profile 284, Carr Inlet (Figure 3a). Solid dots show the inferred base of the Quaternary section. The "a" at top of profile shows inferred active axial plane of folding and dashed shaded lines show boundaries of growth triangle above Rosedale monocline. Gravity profile (solid line) and aeromagnetic profile (dashed line) extracted from Figure 2.

north of Point Defiance (Figure 3). The north and south ends of this profile are about 12 km and 7.5 km farther south, respectively, than those of an overlapping industry seismic reflection profile shown by *Pratt et al.* [1997, their Figure 5]. Mobil 34E images gently north dipping (mean dip < 1.5°) strata in the northern Tacoma basin that are clearly folded upward in the south dipping Rosedale monocline (defining a gentle asymmetric syncline). Two continuous reflectors, "b" and "c," highlight the gentle folding and indicate that there is no significant faulting in this part of the monocline. The maximum dip of reflectors imaging Tertiary strata in the monocline is about 9° to 11° assuming velocities of 3000 to 3500 m/s [*Pratt et al.*, 1997]. Shallower monocline dips, interpreted as apparent dips, occur at the north end of the profile where the seismic profile has a more northerly azimuth and a highly oblique trend to the monocline and gravity gradient. Connecting the traces of the lower hinge of the Rosedale monocline between The Narrows and Carr Inlet reveals that this structure has a northwest trend, parallel to the Gig Harbor gravity gradient.

[41] The rise in Tertiary strata in the Rosedale monocline along the profile corresponds to increases in gravity and magnetism. The short, high-amplitude magnetic anomaly shown above location 10 on Mobil 34E does not correspond to geologic structure and is probably related to a cultural feature.

4.3.2. SHIPS PS-1 and Industry 1 (Figure 10)

[42] SHIPS PS-1 seismic reflection profile extends south through Colvos Passage, then bends about 90° and trends east through Dalco Passage (Figure 3b). Figure 10 also shows a short segment of Industry 1 that overlaps SHIPS PS-1 and provides a better image of shallow structure in an important area. A longer portion of Industry 1 was previously shown by *Pratt et al.* [1997, Figure 5] but with different processing and vertical exaggeration, and without the interpretation in this report. On PS-1, both the north and the east trending line segments are oblique (~45°) to the dip of the Rosedale monocline (Figure 4). The uplift of Tertiary rocks in the Rosedale monocline on both the north and east trending parts of SHIPS PS-1 is associated with increasing gravity and magnetism.

[43] The north trending portion of SHIPS PS-1 shows the upper hinge of the monocline, where south dipping (apparent dips of 11° to 13°) reflectors and gently dipping reflectors are juxtaposed along a steep, north dipping reverse fault ("2"). Industry 1 reveals that this fault and a

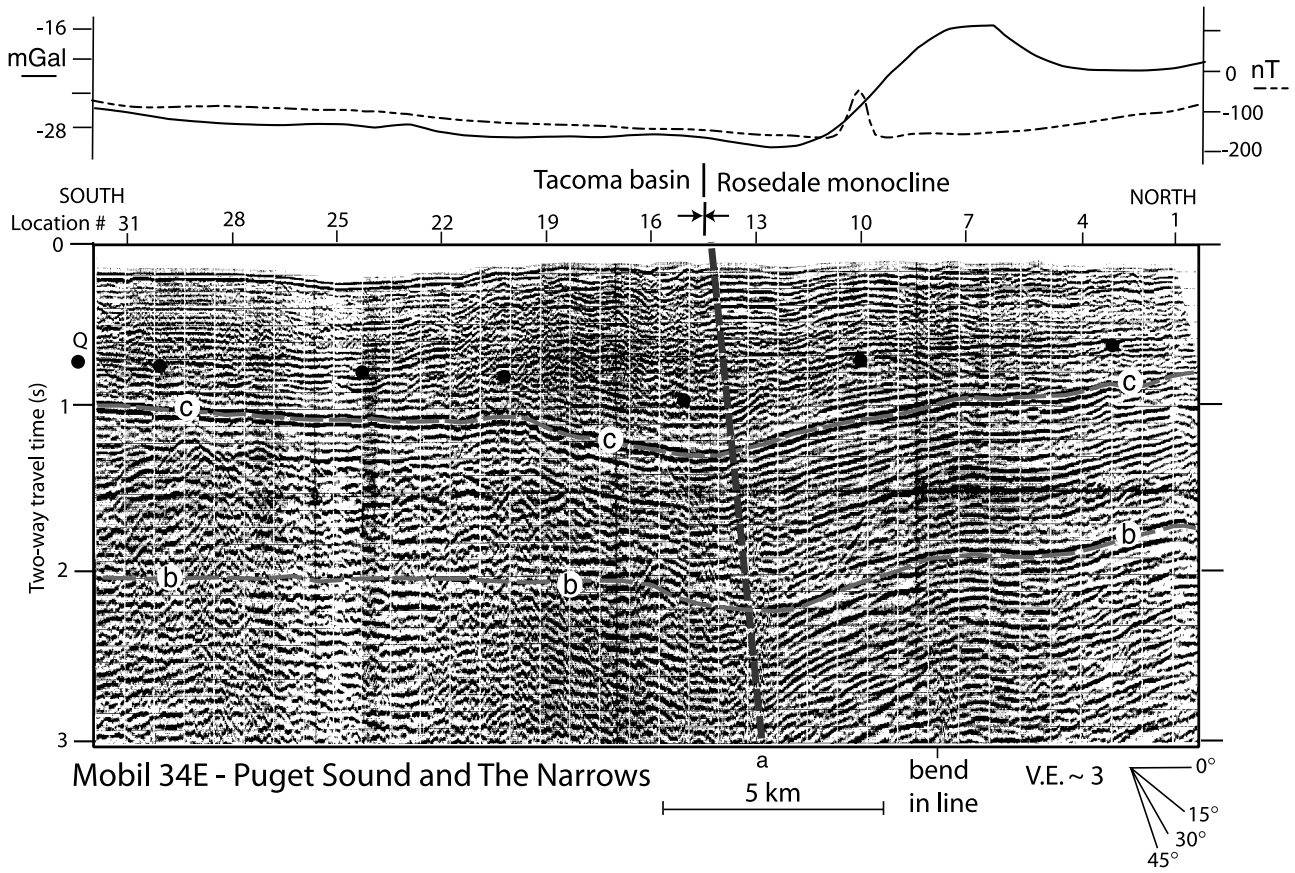

Figure 9. Mobil 34E seismic reflection profile through The Narrows (Figure 3b). Solid dots show the inferred base of the Quaternary section. Dashed lines shows axial plane at base of monocline (“a”), and continuous reflections (“b” and “c”) that highlight the monocline structure. This profile was made available to us only as a degraded paper copy, hence our reproduction is of relatively poor quality. Gravity profile (solid line) and aeromagnetic profile (dashed line) extracted from Figure 2.

south dipping backthrust truncate reflections, appear to terminate upward at about 0.6 to 0.9 s TWTT, and bound a ~2-km-wide antiform that correlates with a prominent magnetic high (Figures 2 and 4). North of the antiform, Tertiary and Quaternary strata are relatively flat (dip < 5°). Industry 1 shows that Quaternary strata are warped above the two faults that bound the antiform. USGS high-resolution seismic reflection data (not shown) reveal warping in the Quaternary section above the southern north dipping fault in this zone but display no obvious shallow disruption associated with the steep northern fault.

[44] SHIPS PS-1 images two additional steep faults: “1a” and “1b.” Reflectors “a” and “b” on PS-1 provide important markers for constraining deformation on these faults as well as structural relief within the Rosedale monocline. Mapping of faults “1a” and “1b” using PS-1 and nearby USGS and industry seismic reflection data strongly suggests they are the same fault, crossed twice by PS-1 as the profile changes from a southerly to an easterly trend (Figure 3b). Fault “1a” appears to displace reflector “a” about 220–280 m (up to the east) whereas reflector “b” at the top of the Tertiary section is continuous above the fault tip. Fault “1b” displaces reflector “a” about 120–180 m up to the south and warps reflector “b” upward into a gentle anticline. Vertical slip on the two images of the fault (~3.5 km apart) thus appears to be reversed on the two crossings, a common characteristic of strike-slip faults [e.g., *Christie-Blick and Biddle*, 1985]. The fault is also imaged on Industry 1 (at km 11.5 in Figure 5 of *Pratt et al.* [1997]), but was not previously interpreted as a fault. There is no evidence on either SHIPS PS-1, Industry 1, or the network of U.S. Geological Survey seismic reflection lines (Figure 3) that this fault significantly deforms Quaternary strata; instead it appears to die out at a depth of about 700 to 1000 m in the uppermost part of the Tertiary section. The fault lies along the trend of the Gig Harbor gravity anomaly and lies along strike with the southwest margin of the oval magnetic high at the head of Commencement Bay (Figures 2 and 4).

4.3.3. U.S. Geological Survey Line 314 (Figure 11)

[45] USGS Line 314 extends east through western Dalco Passage, oblique to the northwest trending Gig Harbor gravity gradient and the two segments of SHIPS PS-1. The unconformity at the base of Quaternary strata is imaged

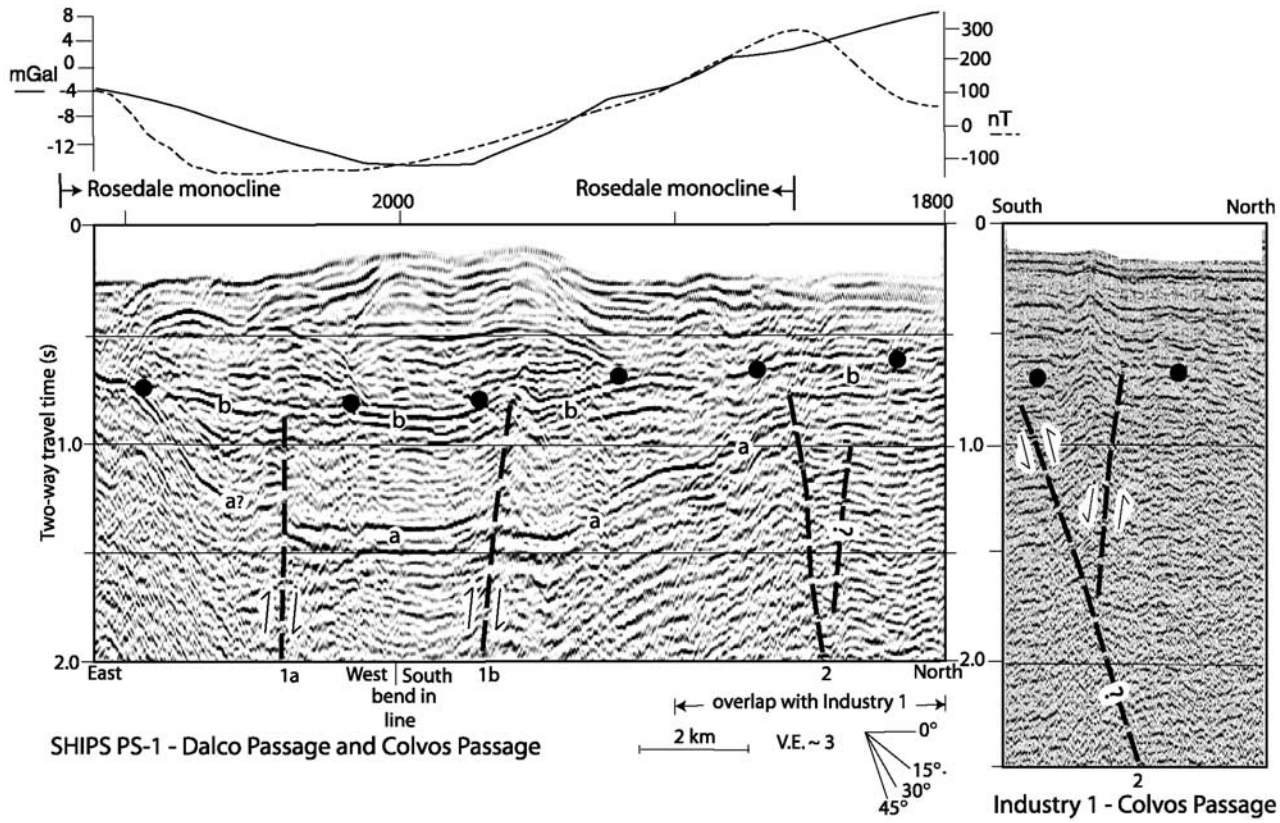

Figure 10. Multichannel SHIPS PS-1 and overlapping single-channel Industry 1 seismic reflection profiles, Colvos Passage and Dalco Passage (Figure 3b). Black dots show the inferred base of the Quaternary section; heavy lines show inferred faults; "a" and "b" show distinctive reflections used as markers to determine fault slip. Portion of single-channel Industry 1 overlaps the northern part of SHIPS PS-2. Gravity profile (solid line) and aeromagnetic profile (dashed line) extracted from Figure 2.

as a high-amplitude reflection in the central part of the line. Below the unconformity, inferred Tertiary strata dip 8° to 10° to the west and have a true dip of ~11°. Quaternary strata imaged in the western part of the line also dip south but at a slightly lower angle (~7°, assuming 1800 m/s). The Quaternary section is essentially horizontal on the eastern part of the line. The hinge between dipping and flat Quaternary strata is analogous to the upper hinge within Quaternary strata imaged in Carr Inlet (Figure 7), and represents the top of the Quaternary part of the monocline (Figure 4).

[46] There is a shallowing of dip within the Tertiary section at about SP 2723, the site where the trace of fault "1a–1b" imaged on SHIPS PS-1 (Figure 10) intersects USGS Line 314. As on SHIPS PS-1, this fault appears to die out within the upper part of the Tertiary section. The uplift of Tertiary strata in the Rosedale monocline correlates with an increase in gravity.

4.3.4. Relevant Geologic Data

[47] *Sherrod et al.* [2002] and B. L. Sherrod (oral communication, 2003) describe 1 to 2 m of late Holocene (~A.D. 980–1190) subsidence at Wollochet (Figure 4), a location that corresponds to the axis of the gentle syncline at the base of the Rosedale monocline imaged on Mobil Line 34E (Figure 9). Nearby in bluffs on the west coast of The Narrows, undated flatlying Quaternary sand and gravel are abruptly warped upward to a 10° southwest dip (Figure 12a); this dip transition represents the hinge at the base of the monocline. Farther north along the west side of The Narrows, there are at least seven sea level exposures of undated Quaternary strata with relatively gentle (<14°) south to southwest dips (Figure 4). Flatlying Quaternary strata higher in the bluffs unconformably overlie these dipping beds.

[48] More highly deformed Quaternary strata crop out in a few isolated tidal zone exposures at Point Evans on the west coast of The Narrows (Figure 4) and in tidal zone and low-bluff exposures along the north and southwest coastline of Point Defiance (S. Boyer and R. E. Wells, oral and written communication, 1996–2002). At Point Defiance, laminated silty mud glaciolacustrine deposits are deformed into gentle north to northeast trending (~350° to 20°) folds (Figure 12b) with wavelengths of a few tens of meters, and strata overlying anticlinal axes are cut by extensional bending-moment faults (Figure 12c).

[49] The Quaternary stratigraphy on the east and west flanks of Colvos Passage (north of Gig Harbor and on

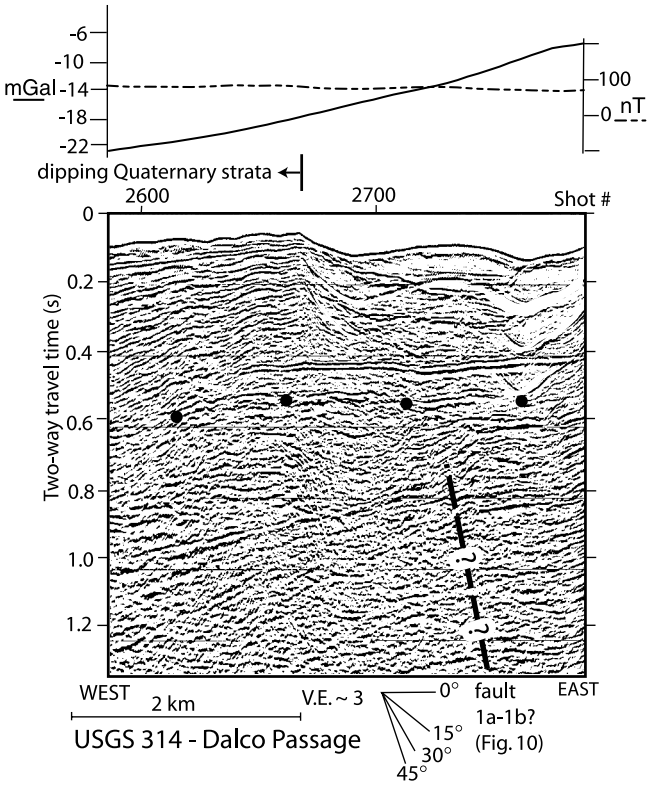

Figure 11. U.S. Geological Survey seismic reflection profile 314, Dalco Passage (Figure 3a). Solid dots show the inferred base of the Quaternary section. Gravity profile (solid line) and aeromagnetic profile (dashed line) extracted from Figure 2.

Vashon Island) opposite SHIPS PS-1 is complex. *Hagstrum et al.* [2002] reported the magnetism of eight samples collected near sea level along this coast and reported four samples with normal polarity, two samples with transitional polarity, and two samples with reversed polarity. That these variably magnetized (and hence variably aged) strata occur at the same elevation suggests large-scale glacial and (or) glaciofluvial scour-and-fill in this area. Faulted, folded, and sheared Quaternary strata occur at Sandford Point (Figure 12d), Camp Sealth, and Olalla (Figure 4), but seismic reflection profiles in Colvos Passage opposite these localities reveal no significant Quaternary faults.

4.3.5. Discussion

[50] Mapping based on seismic reflection data reveals that the Rosedale monocline has a northwest trend (~295–305°) and an approximate width of 11.5 km. Given the approximate monocline dip in The Narrows and Colvos Passage (~10° to 13°), the monocline raises basement about 2.0 to 2.7 km from southwest to northeast. This rise in basement is the source of the northwest trending Gig Harbor gravity gradient (Figures 2 and 10) [*Pratt et al.*, 1977]. The uplift is apparently too gradual, or magnetic strata are too deep, to cause a notable aeromagnetic gradient. The width of the monocline in the Quaternary strata increases significantly from about 4.1 km in Carr Inlet to 6.6 km in The Narrows. Because the dip of the monocline is significantly steeper in Carr Inlet, the amount of Quaternary uplift on the monocline is relatively similar between the two localities. For monocline dips of 16° to 20° in Carr Inlet, the Quaternary uplift is 1.1 and 1.4 km, respectively. For monocline dips of 10° to 13° in The Narrows and Colvos Passage, the Quaternary uplift is 1.2 and 1.5 km.

[51] The inferred fault-bounded uplift in Colvos Passage (Figure 10) coincides with a high-amplitude aeromagnetic anomaly (probably shallow Crescent Formation) which lies on strike with the Allyn magnetic gradient and the Tacoma fault to the west. We therefore infer that the Tacoma fault continues east to Colvos Passage but emphasize that, as it does so, the fault tip becomes deeper and both Quaternary displacement and overall displacement appear diminished. Seismic reflection data suggest that the northwest trending fault imaged in Dalco Passage on SHIPS PS-1 ("1a–1b") appears to die out within the Tertiary section and does not deform Quaternary strata. The approximate coincidence of this structure with both gravity and magnetic anomalies indicates it may have been a more active structure prior to the Quaternary.

[52] As outlined above, deformed Quaternary outcrops in this area (e.g., at Point Defiance and Sandford Point; Figures 4, 12b, 12c, and 12d) do not align with projections of offshore structures and are thus enigmatic. If faults are associated with these exposures, then the amount of vertical displacement is below the resolution (~10–20 m) of the USGS high-resolution seismic reflection data and (or) the faults could have mainly lateral slip which makes them harder to identify on seismic reflection data. Alternatively, some or all of the deformation in these exposures may have a nontectonic origin.

4.4. Dalco Passage, East Passage, and Quartermaster Harbor

4.4.1. SHIPS PS-2 (Figure 13)

[53] SHIPS PS-2 extends northeast from central Dalco Passage through East Passage for about 10 km to offshore of Point Robinson on Maury Island, then bends north and traverses about 5 km through Puget Sound (Figure 3b). At its southwest end, the profile crosses the upper hinge of the Rosedale monocline. Farther northeast, the profile crosses a zone of steep faults and folds that lie east of and along the strike of the Allyn magnetic gradient and the Tacoma fault. Fault "3" juxtaposes more massive, nonreflective material typical of the Crescent Formation on the south and a zone of gently southwest dipping (~8°) reflections more characteristic of Tertiary strata on the north. This inferred south-side-up sense of vertical slip on this steep fault is consistent with interpretations of seismic velocity by A. J. Calvert (written communication, 2001) and with the northward decrease in gravity values. Farther north, faults "4" and "5" are inferred to have opposite, north-side-up, slip based on the hanging wall fold asymmetry. Maximum dip in the panel between faults "2" and "3" is about 11°. Fault "3" is also interpreted as a north dipping reverse or thrust fault based on truncated and mismatched reflectors. The Tertiary sec-

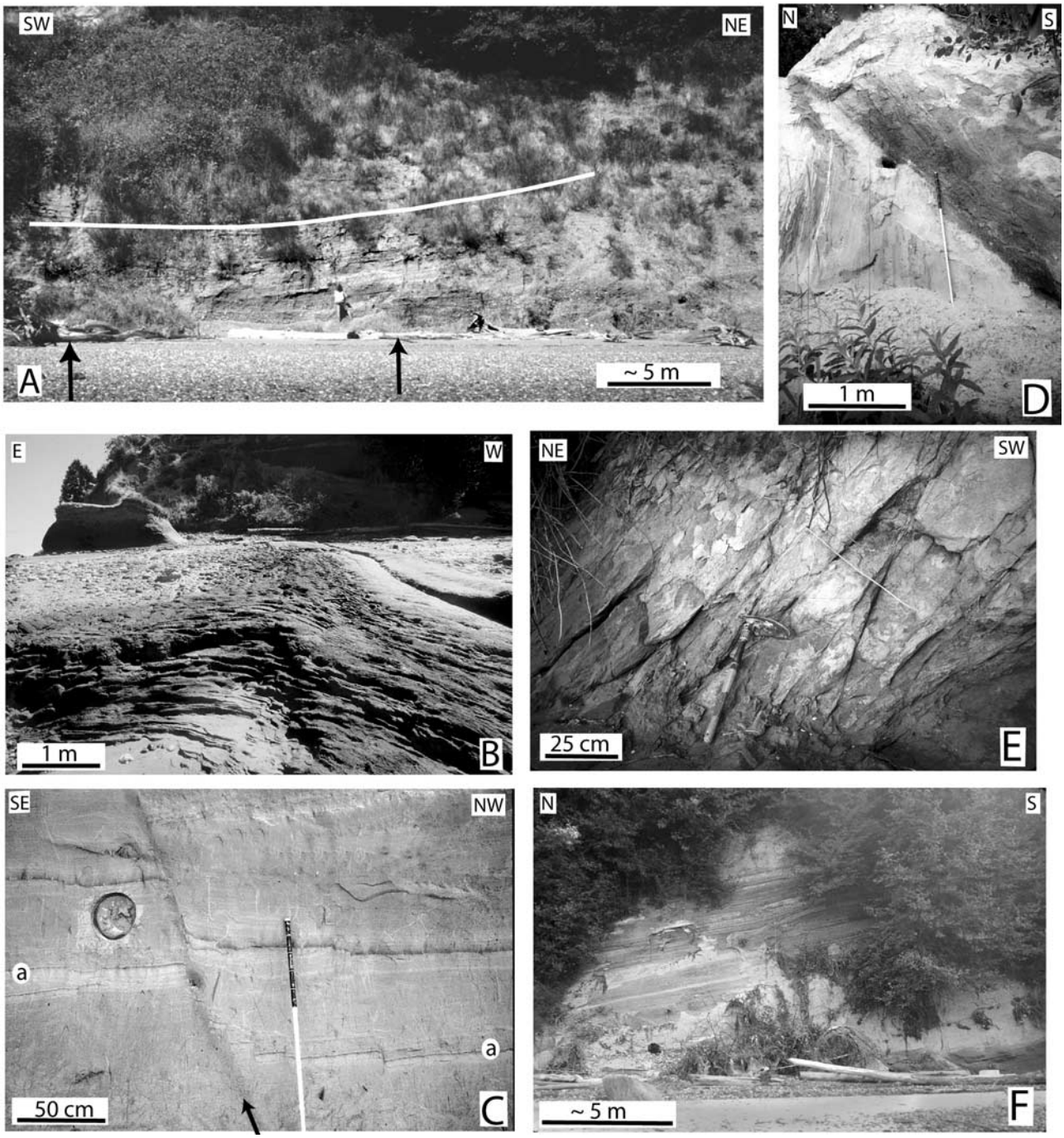

Figure 12. Photographs of coastal bluff exposures in the central Puget Lowland. Locations shown in Figure 4. (a) Quaternary strata south of Point Evans along the west coast of The Narrows, at the lower hinge of Rosedale monocline. Beds above left arrow (left of photo) are flat; beds above right arrow (center of photo) dip south. (b) Axis of outcrop-scale anticline in undated glaciolacustrine deposits, Point Defiance. (c) Normal fault with 35 cm displacement of bed "a," Point Defiance. Numerous comparable structures, interpreted as bending-moment faults, occur above outcrop-scale folds shown in Figure 12b. (d) Thrust fault in undated Quaternary deposits exposed at Sandford Point on southern Vashon Island. Unit in hanging wall (right) is glaciolacustrine pebbly silt; unit at left is plane-bedded glacial outwash sand. (e) Highly fractured, sheared, and destratified sandy and clayey silt, east coast of Quartermaster Harbor. (f) North dipping Quaternary strata (>780 ka?) exposed at Saltwater State Park.

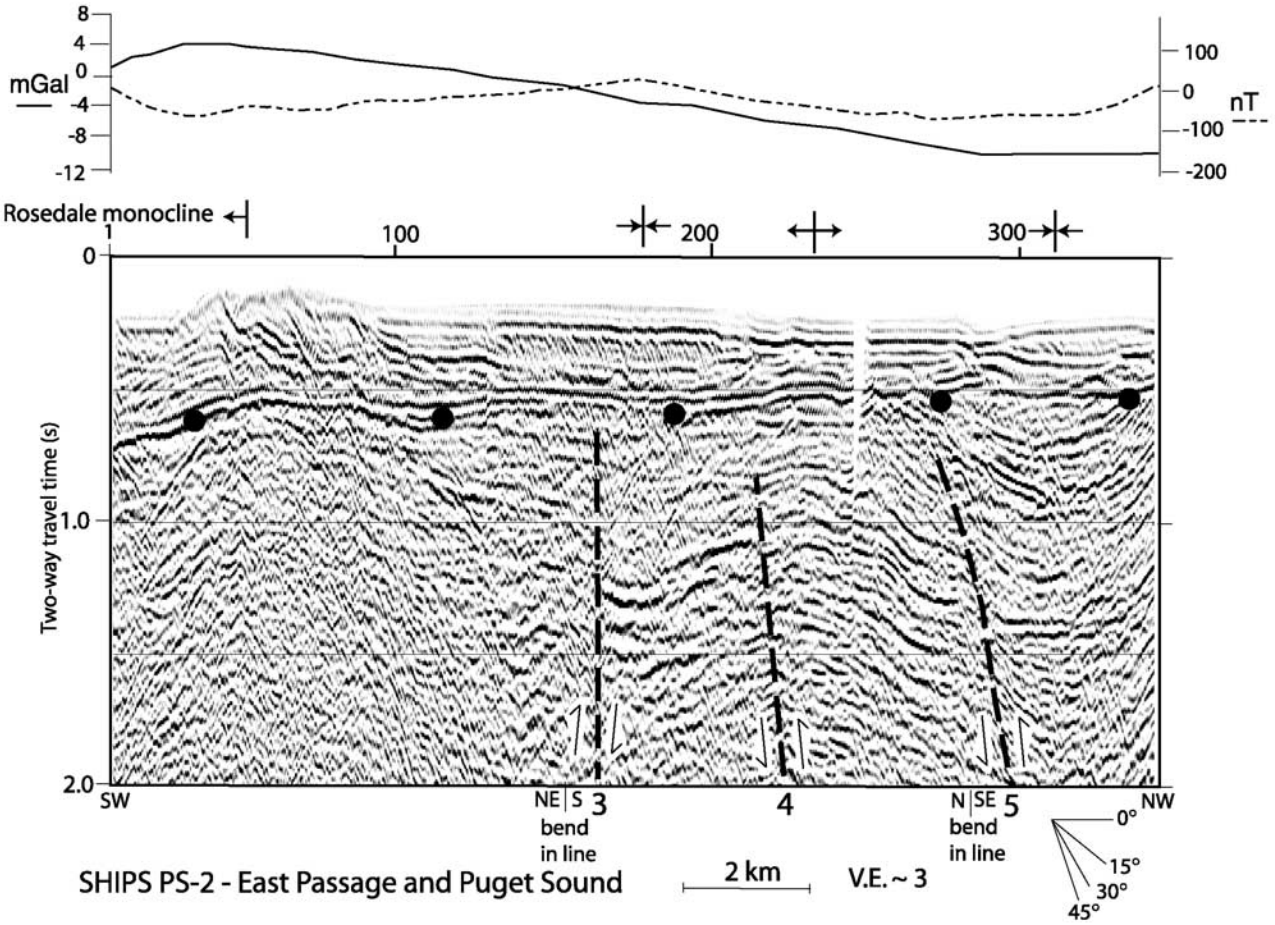

Figure 13. SHIPS PS-2, East Passage and Puget Sound (Figure 3b). Solid dots show the inferred base of the Quaternary section; heavy lines show inferred faults ("3," "4," "5"). Gravity profile (solid line) and aeromagnetic profile (dashed line) extracted from Figure 2.

tion on PS-2 is overlain by Quaternary strata along a prominent angular unconformity. This unconformity is relatively flat and is not obviously disturbed by the underlying faulting and folding.

4.4.2. U.S. Geological Survey Line 205 (Figure 14)

[54] U.S. Geological Survey line 205 extends from offshore Tacoma to offshore Point Robinson (Figure 3), west of and relatively parallel to the southern part of SHIPS PS-2. A prominent pair of high-amplitude reflections that overlie an angular unconformity represents the inferred base of the Quaternary section. At the southwest end of the line, Tertiary strata dip 14°–17° (velocities of 3000–3500 m/s, respectively). Tertiary strata flatten at about shot point 590, the inferred upper hinge of the Rosedale monocline. Uplift of Tertiary beds in the monocline is associated with increased gravity.

[55] Farther northeast, Tertiary strata are folded into an anticline. The anticlinal axis (~shot point 290) is cut by a steep fault that can be traced to fault "3" on SHIPS PS-2 (Figure 13) using other nearby seismic reflection profiles. Fault "4" on line 205 is not well imaged; if present, it is continuous with fault "4" on SHIPS PS-2.

[56] Reflections in inferred Quaternary strata across the profile are hummocky to planar, and have variable amplitude and continuity. Several prominent erosional surfaces truncate reflectors, consistent with a Quaternary history of multiple glaciations and associated glacial and glaciofluvial scour and fill. There is no obvious structural dip (>~2°) in the Quaternary section across the profile, except on the south flank of the faulted anticline where reflections in a ~1300-m-wide panel have an apparent south dip of about 7°. The unconformity at the base of the Quaternary section is relatively flat over most of the profile but dips south (~5°) at the south end of the profile.

4.4.3. U.S. Geological Survey Line 316 (Figure 15)

[57] USGS Line 316 extends north from offshore Tacoma across Dalco Passage into Quartermaster Harbor (Figure 3). The Quaternary section is characterized by discontinuous, locally hummocky, variable amplitude reflections. Numerous low-angle channels are consistent with multiple pulses of glacial and glaciofluvial erosion. The inferred unconformity at the base of the Quaternary section is a moderate to high-amplitude reflection couplet similar to that

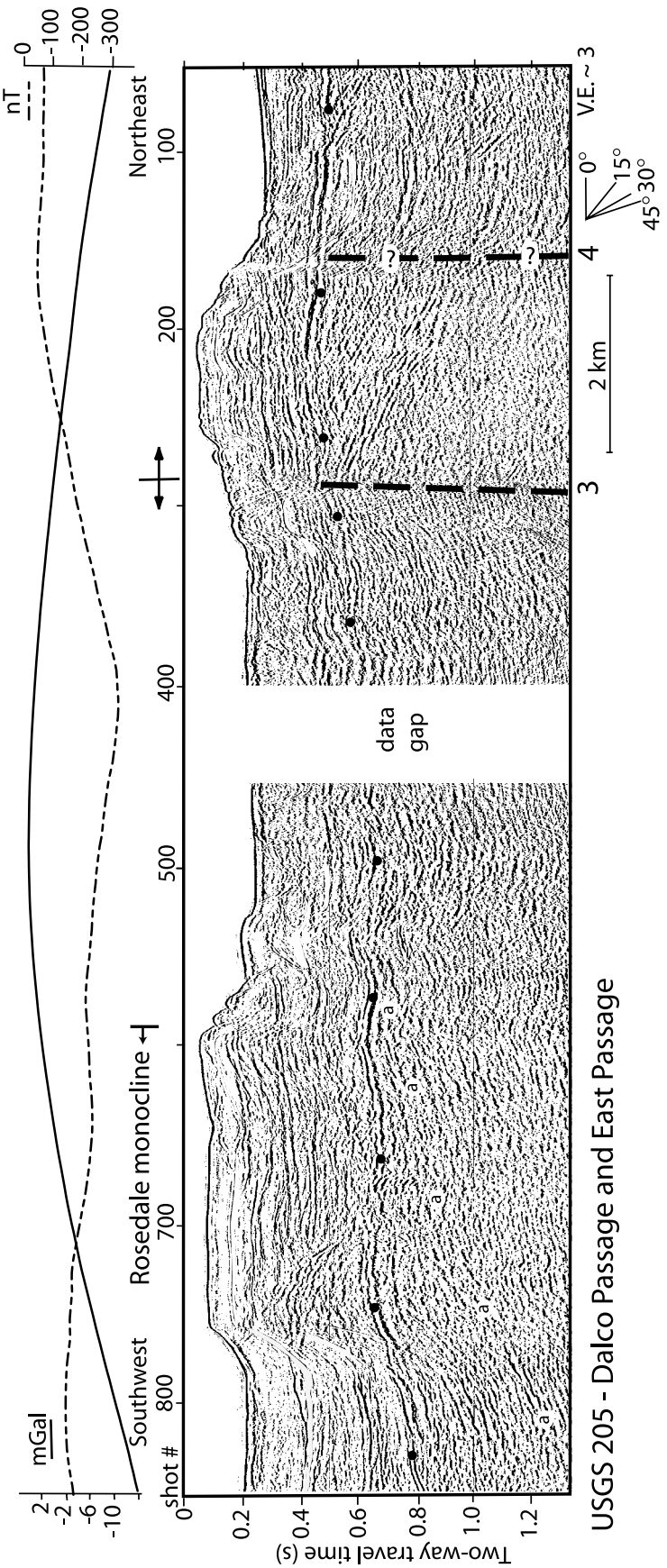

Figure 14. U.S. Geological Survey seismic reflection profile 205, Dalco Passage and East Passage (Figure 3b). Solid dots show the inferred base of the Quaternary section. The ''a'' reflection highlights folding in the Rosedale monocline. Heavy dashed line shows inferred fault. Gravity profile (solid line) and aeromagnetic profile (dashed line) extracted from Figure 2.

seen on lines P205 and P314 (Figures 11 and 14). Overlying Quaternary strata are flat (dip < 1°).

[58] Below the Quaternary unconformity, Tertiary strata are poorly imaged, perhaps due to sideswipe. We map the upper hinge of the Rosedale monocline at about shot point 520. South of this point, Tertiary strata have an overall south dip but are gently folded into an anticline and syncline with limb dips of about 5° to 7° (highlighted by reflector "a"). The gentle folds cannot be traced onto adjacent lines and are inferred to be minor structures with limited lateral extent. North of the projected hinge of the Rosedale monocline, Tertiary strata are flat. As along other profiles, an increase in gravity is associated with uplift of Tertiary strata in the monocline.

4.4.4. Relevant Geologic Data

[59] Seismic reflection profiles in Quartermaster Harbor (Figures 3 and 15) do not clearly reveal Quaternary deformation. Hence, faults that might connect the deformation in East Passage with that in Colvos Passage and farther west must either lie north of the seismic survey or deeper than the stratigraphic level imaged in Figure 15 (~1 km). Quaternary strata exposed on the flanks of Quartermaster Harbor and East Passage provide a potential test of the hypothesis that the east trending Tacoma fault structural zone extends east across Puget Sound waterways to the mainland.

[60] Outcrops along the northwestern shore of Quartermaster Harbor on Vashon Island consist of massive till or are of such poor quality that they provide no data to test the faulting hypothesis. Along the northeastern shore of the harbor (on western Maury Island), highly fractured, sheared, and destratified sandy and clayey silt (Figure 12e) occur discontinuously along the base of the coastal bluff for about 170 m (Figure 4), consistent with eastern continuation of the Tacoma fault. Fractures generally strike 95° to 110° and dip 45° to 70°N. The eastern projection of this structural zone intersects the east coast of Maury Island in an area of extensive landsliding and poor exposure where there is no evidence for or against eastward continuation of the Tacoma fault.

[61] The zone of deformation imaged on Figure 13 between faults "3" and "4" can be traced with seismic reflection data across East Passage, projecting onland at Saltwater State Park (Figure 4) where there is considerable evidence for deformation in Quaternary deposits exposed along the coastal bluffs and in the wave-cut bench. These strata yielded reversed magnetic polarities and are probably older than 780 ka [*Hagstrum et al.*, 2002]. In the southern part of the park, a 200-m-wide section of distinctive alluvial sand and silt strikes 95° and dips as steeply as 16° north. A distinctly different stratigraphic section, consisting of sand-gravel outwash, till, and interglacial sand, silt, and peat, occurs in the northern part of Saltwater State Park. These beds locally dip as steeply as 13–15° and are cut by a subvertical southeast trending (140°) fault with an estimated 8 m of slip, numerous east-southeast (100°–125°) fractures, sand-filled dikes, and gravel-filled extensional cracks. The contact between the strata exposed in the southern and northern parts of the park is not exposed but is a suspected fault based on the stratigraphic mismatch and on the abundant nearby deformation.

[62] Farther north, deformed Quaternary strata exposed at Normandy Beach Park coincide with the zone of deformation along fault "3" on Figure 13. Sand and gravel beds dip as steeply as 20° to the south, and are cut by a normal fault (attitude of 65°, 56°NW) with 50 cm of slip and numerous northeast trending (27°to 60°) fractures.

[63] The amount of deformation in these exposures is thus larger than the amount of Quaternary deformation detectable on seismic reflection profiles in East Passage (Figures 13 and 14). It may be that much of the strata imaged on these profiles is of late Quaternary age (100 ka or much less) and therefore postdates much of the potentially older deformation noted at Saltwater State Park and Normandy Beach Park.

4.5. Discussion

[64] Information from Dalco Passage, East Passage, and Quartermaster Harbor confirm the presence of the Rosedale monocline coincident with the Gig Harbor gravity gradient. The monocline has a total width of about 11.5 km; the width of dipping Quaternary strata in the monocline is about 6.6 km.

[65] Seismic reflection and geologic data are consistent with a zone of deformation, here referred to as the "East Passage zone," extending across Vashon Island, Maury Island, and East Passage. Fault "4" (Figures 4, 13, and 14) is on strike with and has similar geometry to the Tacoma fault to the west, and may be an eastern segment of that fault. We choose, however, to refer to the Tacoma fault and East Passage zone as separate features until that hypothesis has been more fully documented.

[66] A structure comparable to fault "3" in the East Passage zone does not appear to be present farther to the west along the Tacoma fault trend. Because of its inferred steep dip and south-side-up slip, we suspect fault "3" may be primarily a strike-slip fault. In this scenario, the East Passage zone is an oblique slip zone in which thrusting and strike-slip motions are partitioned on different structures.

[67] As noted above, aeromagnetic and (or) gravity gradients do not obviously coincide with the East Passage zone (Figure 2). Fault "3" on Figure 13 does occur on the northern margin of a prominent oval-shaped aeromagnetic low in eastern East Passage but, farther east, it runs across rather than parallel to the aeromagnetic gradient. The lack of an aeromagnetic expression for this fault and for faults "4" and "5" on Figure 13 may reflect one of or a combination of the following factors. (1) Near-surface Crescent Formation in this portion of the Seattle uplift is reversely magnetized [*Hagstrum et al.*, 2002]. The inverse correlation of gravity and magnetic data along the seismic profiles in Figures 13 to 15 is consistent with this inference. (2) Faulting in the west juxtaposes the Seattle uplift and Tacoma basin. Faulting in the east is within the Seattle uplift where the Crescent Formation is close to the surface on both sides of the fault. (3) There is significantly less vertical displacement on this eastern part of the fault than on segments to the west. (4) Deformation to the west extends upward to the near surface and surface and may be locally characterized

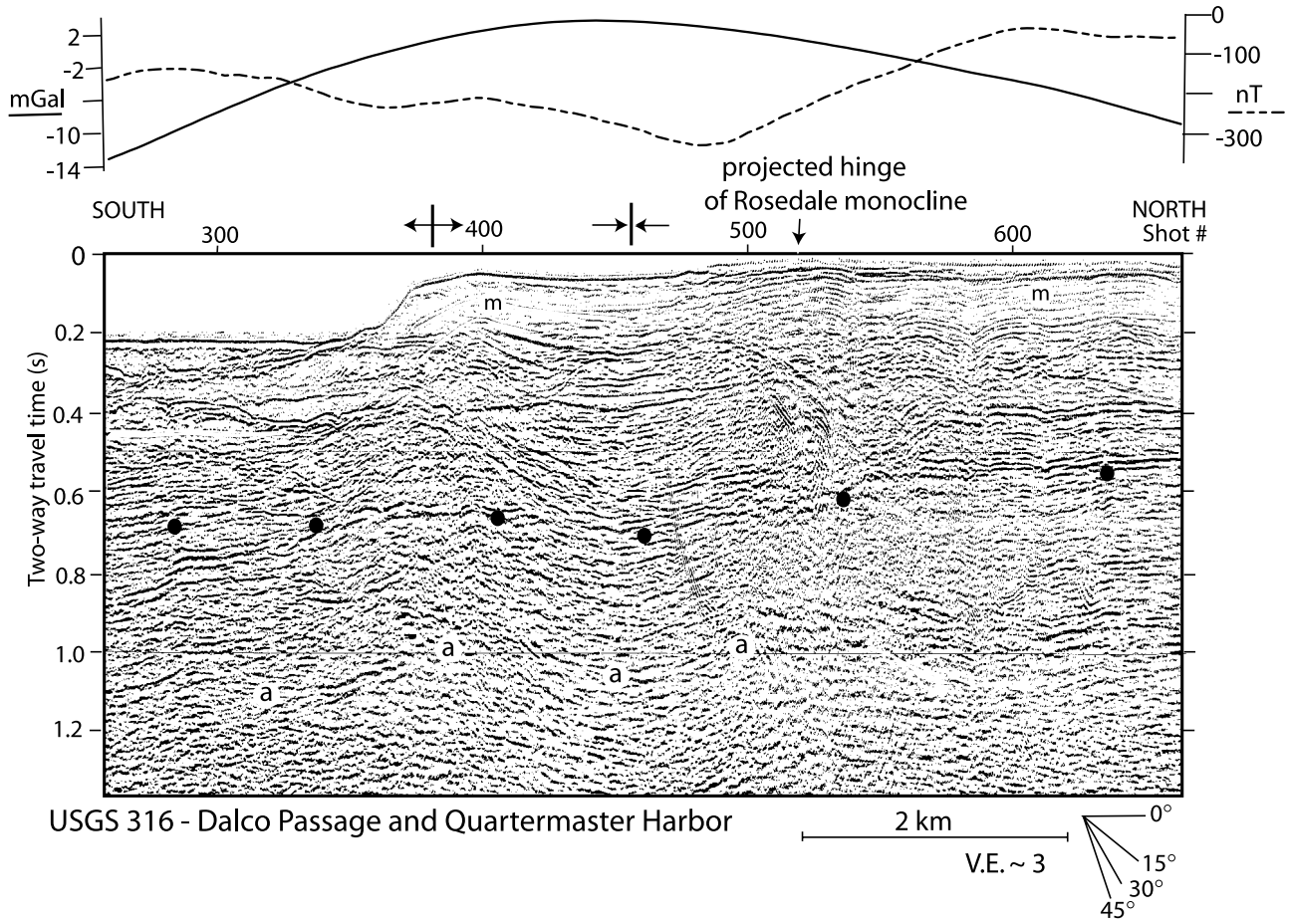

Figure 15. U.S. Geological Survey seismic reflection profile 316, Dalco Passage and Quartermaster Harbor (Figure 3a). Solid dots show the inferred base of the Quaternary section. The "a" reflection highlights folding beneath the Tertiary-Quaternary unconformity. The "m" shows water-bottom multiples. Gravity profile (solid line) and aeromagnetic profile (dashed line) extracted from Figure 2.

by surface faulting; deformation to the east is deeper and characterized more by folding.

5. Structure of the Northern Margin of the Tacoma Basin

[68] *Pratt et al.* [1997] suggested that the northern and northeastern margin of the Tacoma basin are characterized by a northwest trending monocline. This hypothesis is consistent with all of the geophysical and geologic data we present from Carr Inlet eastward. However, seismic reflection data do not image a monocline farther to the west near Case Inlet (Figures 4, 5, and 6), where the basin margin has a westerly trend based on the gravity and magnetic anomalies (Figure 2), seismic tomography [*Brocher et al.*, 2001], and structure contours. If the monocline does continue to the northwest of Carr Inlet, then the lower hinge of the monocline must lie north of and beneath the tip of the Tacoma fault.

[69] On the basis of the seismic tomography, which shows a large velocity gradient along the western part of the Tacoma basin margin, *Brocher et al.* [2001] suggested that the entire basin margin is defined by a steep, north to northeast dipping fault that follows both the west trending western segment and the northwest trending eastern segment of the Gig Harbor gravity gradient. However, the tomography data do not show a steep velocity gradient east of Carr Inlet, and no significant, northwest trending, basin-margin fault was imaged on seismic reflection data in Carr Inlet (Figure 4). The absence of smaller-scale southwest vergent folding within the monocline (similar to that imaged in Case Inlet; Figures 6 and 7) argues against the hypothesis that a northeast dipping, blind, basin-margin fault underlies the eastern northwest trending segment of the Gig Harbor gravity gradient. Additionally, the notion that the entire Rosedale monocline is the forelimb of a fault propagation fold formed above a blind northeast dipping fault is highly unlikely because of the ~11.5 km width of the monocline, the shallow dip (10°–20°) of the monocline, and the lack of a fold backlimb (Figures 13 and 14). Alternatively, the observed flat and monocline geometry imaged by seismic reflection profiles in Carr Inlet and areas to the east is consistent with the fault–bend fold deformation model [*Suppe*, 1983] proposed by *Pratt et al.* [1997].

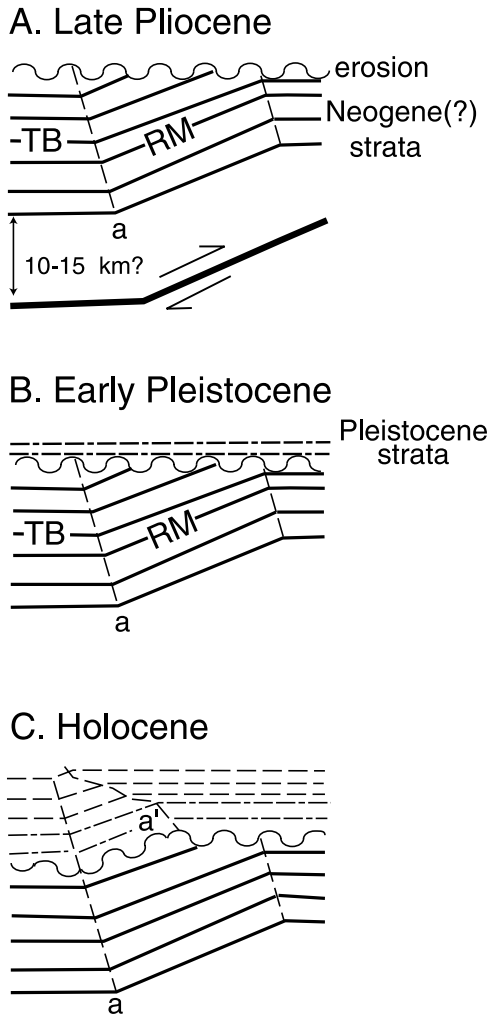

Figure 16. Fault-bend fold model for origin of the Rosedale monocline (RM) based on U.S. Geological Survey line 272 in Carr Inlet (Figure 8). (a) End of Pliocene. Tertiary strata of the Tacoma basin (TB) have been folded above a bend in a deep (15–20 km?) underlying thrust fault, forming a monocline. Folded beds are beveled by erosion associated with drop of sea level and onset of glacial ages. The "a" is the active axial surface. (b) Early Pleistocene. Pleistocene strata are deposited over folded Tertiary strata with angular unconformity. Tertiary-Quaternary contact becomes disconformable north and south of the monocline. (c) Pleistocene strata transported north across lower monocline hinge are folded, forming kink band and growth triangle between active (a) and inactive (a′) axial surfaces. Irregular shape of growth triangle reflects variable sedimentation and erosion rates associated with multiple pulses of Pleistocene glaciation.

[70] Application of the fault-bend fold model provides important insights and constraints for understanding late Tertiary and Quaternary deformation. For example, Figure 16 shows the structural evolution of the Carr Inlet area based on U.S. Geological Survey line 272 (Figure 7). In Figure 16a, Tertiary strata in the monocline are folded above a ramp in an underlying thrust fault, then beveled by a latest Tertiary to earliest Quaternary erosion surface. "a" is the active axial surface of folding at the base of the monocline. Lower Pleistocene strata are then deposited over Tertiary strata above the ramp (Figure 16b) and in the Tacoma basin; the contact is an angular unconformity over the ramp and a disconformity north and south of the ramp. Pleistocene strata of the Tacoma basin become folded as they are tectonically transported through the active axial surface (Figure 16c). With ongoing tectonic transport and deposition in the Tacoma basin, folded Pleistocene beds form an upward narrowing growth triangle [*Suppe et al.*, 1992]. As described in the next section, the scale of the growth triangle provides an indication of the amount of Quaternary tectonic transport and fault slip rate. The shape of the growth triangle (narrowing rapidly at the top) suggests irregular depositional rates with a significant thickness of latest Pleistocene (Vashon?) strata or, less likely, the ending of folding in the middle to late Pleistocene.

[71] Different structural interpretations of the central Puget Lowland are summarized in Figure 17. The interpretations of this report (Figures 17b, 17d, and 17f) assume but modify the thrust-sheet hypothesis of *Pratt et al.* [1997] (Figure 17e). In addition to the arguments for thrusting presented by Pratt et al., crustal shortening in the central Puget Lowland is supported by seismic reflection and refraction data reported by *ten Brink et al.* [2002], which indicate a dip on the Seattle fault of about 35°to 45° down to a depth of 7 km. This geometry is consistent with evidence from seismic reflection data reported by *Johnson et al.* [1994, 1999], *Pratt et al.* [1977], *Calvert et al.* [2001, 2003], and unpublished industry data, all of which also reveals significant folding. There is also significant evidence for crustal shortening in outcrops. Quaternary strata on the Seattle uplift locally dip 5° to 20° (Figures 4 and 12; D. B. Booth and K. G. Troost, oral communication, 2000). Mapping [*Yount and Gower*, 1991] and trenching [*Nelson et al.*, 2002, 2003a, 2003b] in the Seattle fault zone reveal tightly folded and overturned Eocene to Miocene strata and low-angle, north dipping backthrusts. The scale and geometry of this contractional deformation is inconsistent with master faults dipping >70°. To produce this shortening along such steep faults would result in far more uplift and relief in the Puget Lowland than presently exists.

[72] Given the above, our preferred interpretation (Figures 17b, 17d, and 17f) is that the northern margin of the Tacoma basin has a compound origin and that elements of both the models of *Pratt et al.* [1997] and *Brocher et al.* [2001] are correct. Our eastern cross section (B-B′; Figure 17d) is similar to that of Pratt et al. (Figure 17e), but it shows part of the Seattle uplift as a structural "pop-up" as first suggested by *Brocher et al.* [2001], bounded by the Seattle fault and north dipping faults in the East Passage zone. ("Pop-up" is used after *McClay* [1992] to describe a section of hanging wall that has been uplifted by the combination of a foreland-vergent thrust and a hinterland-vergent thrust.) Considerable contractional deformation clearly has occurred on both north and south dipping faults

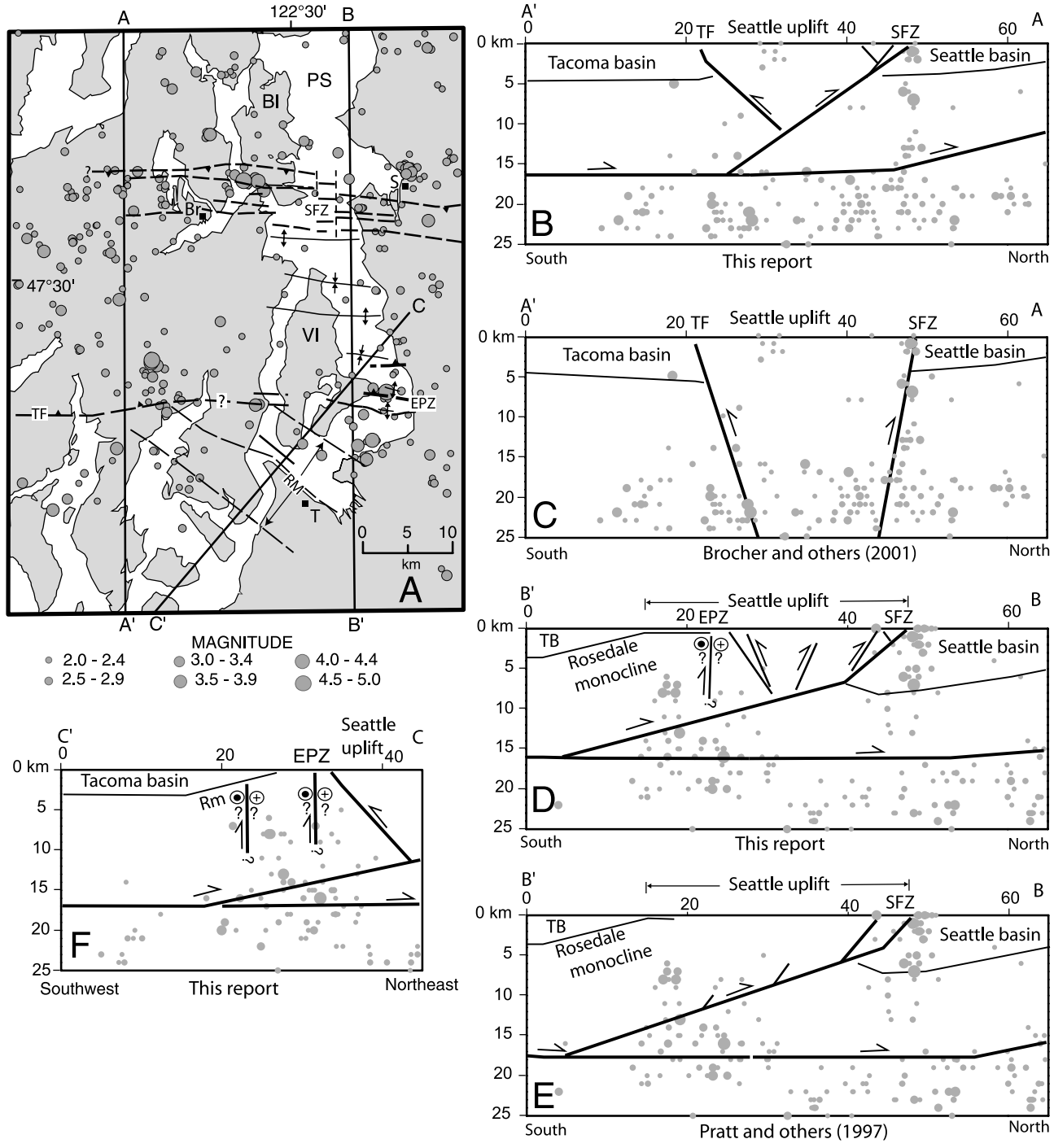

Figure 17. (a) Schematic map and (b, c, d, e, and f) cross sections along lines A-A′, B-B′, and C-C′ showing different structural interpretations for the central Puget Lowland and seismicity. Hypocenters are from the Pacific Northwest seismic network for the years 1970–2001 and have magnitude ≥2 and depth uncertainty of up to ~4 km. Swaths of hypocenters projected onto cross-section lines are 25 km wide. BI, Bainbridge Island; Br, Bremerton; EPZ, East Passage zone; PS, Puget Sound; RM, Rosedale monocline; S, Seattle; SFZ, Seattle fault zone; T, Tacoma, TF, Tacoma fault; VI, Vashon Island.

and associated folds within the Seattle uplift, but the manner in which these faults interact with each other and the master thrust at depth is poorly constrained. Faults in the East Passage zone have shallow basement on both flanks, and probably have much less vertical displacement than the Tacoma fault farther west.

[73] Our western cross section (A-A′, Figure 17b) is consistent with *Brocher et al.* [2001] (Figure 17c) in that we show the entire Seattle uplift as a structural pop-up bounded to the south by the Tacoma fault. We infer that the steep fault dip inferred from Figure 6 shallows with depth and that the Rosedale monocline continues its northwest trend and lies entirely in the footwall of the Tacoma fault. Structural relief on the Tacoma basin margin in this region is greater than to the east. Conversely, gravity data (Figure 2) suggest that structural relief on the western part of the Seattle fault is less than to the east. *Brocher et al.* [2001] first noted this relationship and suggested that regional shortening is partitioned between the Seattle fault and Tacoma fault in this part of the Puget Lowland.

[74] The role of lateral slip in the structural evolution of the south flank of the Seattle uplift is unknown but potentially significant. The steep, northwest trending fault in Dalco Passage (fault "1" on Figures 4 and 10) connects with and is parallel to the Gig Harbor gravity gradient and could have far more lateral slip than the few hundred meters of noted vertical slip. Similarly, we think fault "3" in the East Passage zone could have significant lateral slip, and the positive flower structure in Case Inlet (Figure 5) also suggests lateral slip. Regional deformation patterns based on geology and geophysics [e.g., *Johnson et al.*, 2001] as well as recent GPS-based deformation models [e.g., *Khazaradze et al.*, 1999; *Miller et al.*, 2001; *Mazotti et al.*, 2002] suggest left-lateral slip is most likely.

[75] Figure 18 shows two models in which the crustal shortening direction for the central Puget Lowland varies from north (Figure 18a) to northeast (Figure 18b) and the geometry and style of oblique-slip or strike-slip faulting varies. In Figure 18a, tectonic transport along the inferred thrust fault beneath the Rosedale monocline is to the north, oblique to the trend of the monocline. In this scenario, the monocline could overlie an oblique ramp in the underlying thrust, or its northwest trend could be relict from a precursor stress regime. North-south shortening favors north directed thrusting on west trending structures such as the Seattle and Tacoma faults, and left-lateral strike slip is favored on northeast trending faults such as the inferred structure on the northwest flank of the Dewatto basin. Given this scenario (Figure 18a), it is possible that the Dewatto basin formed as a small pull-apart basin associated with transfer of slip between two diverging high-angle faults. The inferred north and northeast trending faults bounding the Dewatto basin form significant geophysical lineaments [*Blakely et al.*, 1999; *Brocher et al.*, 2001] but have not been verified with detailed local geologic or geophysical information.

[76] Figure 18b shows an alternative interpretation in which the shortening direction is northeast, normal to the Rosedale monocline. In this scenario, east-west structures

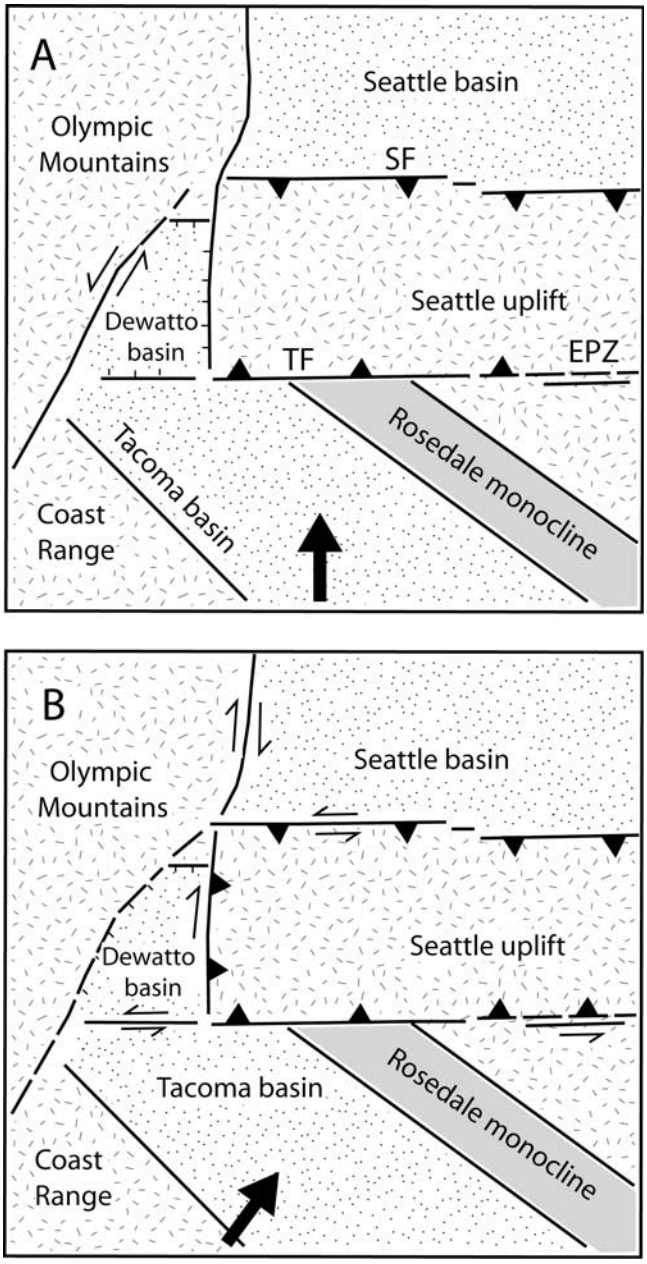

Figure 18. Schematic diagrams showing different hypotheses for structural deformation in the central Puget Lowland based on different principal shortening directions, indicated by bold arrows: (a) north-south shortening; (b) northeast-southwest shortening.

such as the Seattle and Tacoma faults are characterized by north-south shortening and a lesser component of left-lateral slip. Also, deformation in the East Passage zone (Figure 13) is partitioned into thrust or reverse faults (faults "4" and "5") and a strike-slip fault (fault "3"). The Dewatto basin could have formed through a combination of thrust loading on its eastern basin margin, transfer of right-lateral slip between north and northeast trending faults, and transfer of left-lateral slip from the Tacoma fault to the Seattle fault.

[77] Geologic, geophysical, and geodetic data from the central Puget Lowland are thus consistent in that they indicate north or northeast directed crustal shortening. At this time, it is difficult to determine whether the different trends of contractional structures indicate local variations in thrust geometry and (or) the stress field, the effects of crustal heterogeneity and relict structural grain, or some combination of the above. Some specific tests of the above hypotheses could involve examination of the Seattle and Tacoma faults for evidence of left-lateral slip, and investigation of the structures on the flanks of the Dewatto basin.

6. Seismicity and Earthquake Hazards

[78] The regional seismicity catalog does not provide information sufficient to constrain tectonic models. Figure 17 shows that most crustal seismicity beneath the Puget Lowland occurs at depths of 15 to 25 km and is widely scattered both in map view and cross section. Although depth uncertainties (2–4 km) make any interpretation questionable, we infer that some of the earthquakes in this seismogenic zone occur in a band along the master decollement of *Pratt et al.* [1997] that links to the Seattle fault. Other lower-crustal earthquakes may occur in weaker portions of the Crescent Formation, perhaps within sedimentary or volcaniclastic horizons. Shallow portions (above ~15 km) of the Seattle fault, the Seattle uplift, the Tacoma fault, and the Tacoma basin are essentially aseismic. The Seattle basin experienced a recent swarm of shallow earthquakes, initiated by the 6/23/97 M 4.9 Bremerton earthquake which we infer is related to an intrabasinal normal fault stressed by the hanging wall of the Seattle fault [*Blakely et al.*, 2002].

[79] *Brocher et al.* [2001] noted the apparently synchronous uplift at ~A.D. 900 along both the Seattle fault and the Tacoma fault [*Bucknam et al.*, 1992] (Figure 4), and the contrasting trend in structural relief along the Tacoma fault (more to the west) and Seattle fault (more to the east). They interpreted these observations as linked slip between the Seattle and Tacoma faults. This hypothesis is consistent with the cross sections of Figures 17b and 17d, which suggest that movement on a master thrust could result in synchronous shallow displacement on either the Tacoma fault, the Seattle fault, or on both.

[80] *Pratt et al.* [1997] used the width of the Rosedale monocline to estimate the total amount of slip on the master thrust fault since its inception. Of more importance is the amount of fault slip during the Quaternary, which (assuming the structural model is correct) can be inferred from the ~4.1 km (Carr Inlet) to 6.6 km (The Narrows to Dalco Passage) width of the panel of dipping Quaternary strata on the monocline (Figures 4 and 16). Dividing these two widths by 2 Ma, the assumed age for the onset of Quaternary deposition, yields a slip rate of ~2.1 to 3.3 mm/yr. Given the shallow dips on the monocline, the rate of shortening is only slightly less than the rate of slip, about 2 to 3 mm/yr.

[81] These estimated rates indicate that a significant portion of the estimated 4–6 mm/yr of northward shortening suggested by GPS models [*Khazaradze et al.*, 1999; *Miller et al.*, 2001; *Mazotti et al.*, 2002] for western Washington is accommodated in the central Puget Lowland between the Tacoma fault and the Seattle fault (Figure 1). *Johnson et al.* [1999] previously suggested a slip rate of about 0.7 to 1.1 mm/yr for the Seattle fault and a shortening rate of about 0.4 to 0.7 mm/yr assuming a 50° dip in the upper kilometer of the crust. However, this estimate was largely based on the "Frontal fault" [*Blakely et al.*, 2002] in the broad Seattle fault zone, and precedes significant awareness of the presence and history of backthrusting [e.g., *Nelson et al.*, 2002, 2003a, 2003b]. Hence the previous estimates of *Johnson et al.* [1999] for the Seattle fault zone should be considered as minimum values.

[82] The difference between the actual shortening within the Seattle fault zone (>1 mm/yr?) and the estimated 2 to 3 mm/yr on the master thrust must be accommodated by shortening on other structures such as the Tacoma fault. Along the western part of the Tacoma fault near Case Inlet, the amount of structural relief on the base of the Quaternary suggests minimum slip and shortening rates of 0.19 and 0.06 mm/yr, respectively, assuming a fault dip of about 71° in the upper few kilometers (Figure 6). As discussed above, analysis of geologic and geophysical data indicates that slip on the Tacoma fault decreases eastward. This suggests that significant Quaternary deformation has occurred elsewhere between Seattle and Tacoma. Put differently, we infer that the crustal deformation between Seattle and Tacoma is all forced by slip on the deeper Seattle fault, and that the portion of this slip not recorded by deformation in the shallow Seattle fault zone is distributed on the Tacoma fault, East Passage fault zone, and other structures beneath the Seattle uplift. Future work should focus on further identifying and documenting the slip on these structures, so that their significance can be considered in seismic hazard assessment [e.g., *Frankel et al.*, 1996, 2002].

7. Conclusions

[83] Synthesis of the tectonics of the south central Puget Lowland portion of the Cascadia forearc provides an important case history for understanding margin-parallel shortening and earthquake hazards in oblique convergent continental margins. Integration of information from seismic reflection surveys, coastal exposures of Pleistocene strata, potential-fields data, and airborne laser swath mapping has been essential for documentation and interpretation of the structural boundary between the Seattle uplift and the Tacoma basin in Washington's central Puget Lowland. This boundary is a complex structural zone characterized by two distinct segments. The northwest trending eastern segment, extending from Tacoma to Carr Inlet, is formed by the ~11.5-km-wide, southwest dipping, Rosedale monocline. This monocline raises basement about 2.5 km, resulting in a moderate gravity gradient. We interpret the Rosedale monocline as a fault-bend fold, forming above a ramp on a deeper thrust fault. Within the Rosedale monocline, inferred Quaternary strata thin northward and form a growth triangle that is 4.1 to 6.6 km wide at its base, suggesting

~2–3 mm/yr of slip on the underlying thrust. This slip must be accommodated by structures in the central Puget Lowland, including the Seattle fault, the Tacoma fault, and structures within the Seattle uplift.

[84] The western section of the north dipping Tacoma fault, extending from Hood Canal to Carr Inlet, forms the western segment of the Tacoma basin margin. Structural relief on this portion of the basin margin may be as much as 5 to 7 km, resulting in steep aeromagnetic, gravity, and velocity anomalies. Quaternary structural relief along the western Tacoma fault is as much as 360 m, indicating a minimum slip rate of about 0.2 mm/yr.

[85] East of Carr Inlet, the Tacoma fault extends to Colvos Passage and probably across Vashon Island and East Passage to Saltwater State Park. This eastern fault section is marked by less distinct geophysical anomalies, diminished structural relief, distributed deformation over a width of a few km, and a probable component of oblique slip. The Tacoma fault and north dipping faults in the East Passage zone are inferred to be north dipping backthrusts to the Seattle fault, making the Seattle uplift a "pop-up" structure. In this model, slip on a master thrust fault at depth could result in movement in the Seattle fault, the Tacoma fault, the East Passage zone, or other structures within the Seattle uplift.

[86] **Acknowledgments.** This work was funded jointly by Earthquake Hazards Reduction Program and Coastal and Marine Geology programs of the U.S. Geological Survey. We thank Jon Childs, Walter Barnhardt, Kevin O'Toole, Larry Kooker, Fred Payne, Curtis Lind, and the captain and crew of the *MV Robert Gray* for help in data collection. We are grateful to Mobil for providing industry seismic reflection data. We thank Susan Rhea for GIS support. We benefited from many discussions with John Armentrout, Derek Booth, Thomas Brocher, Robert Bucknam, Carol Finn, Arthur Frankel, Jon Hagstrum, Ralph Haugerud, Robert Karlin, William Lingley, Thomas Moore, Christopher Potter, Thomas Pratt, Brian Sherrod, Uri ten Brink, Kathy Troost, Timothy Walsh, Craig Weaver, Ray Wells, and James Yount. Thomas Pratt, Thomas Brocher, and Brian Wernicke provided stimulating and helpful reviews.

References

Aber, J. S. (1993), Glaciotectonics and mapping glacial deposits, 309 pp., Can. Plains Res. Cent., Regina, Saskatchewan, Canada.

Aber, J. S., D. G. Croot, and M. M. Fenton (1989), Glaciotectonic landforms and structures, 200 pp., Kluwer Acad., Norwell, Mass.

Abers, G., and R. McCaffrey (1988), Active deformation in the New Guinea fold-and-thrust belt: Seismological evidence for strike-slip faulting and basement-involved thrusting, *J. Geophys. Res.*, *93*, 13,332–13,354.

Ave Lallemant, H. G. (1996), Displacement partitioning and arc-parallel extension in the Aleutian volcanic island arc, *Tectonophysics*, *256*, 279–293.

Babcock, R. S., R. F. Burmester, D. C. Engebretson, and A. Warnock (1992), A rifted margin origin for the Crescent basalts basalts and related rocks in the northern Coast Range volcanic province, Washington and British Columbia, *J. Geophys. Res.*, *97*, 6799–6821.

Blakely, R. J., R. E. Wells, and C. S. Weaver (1999), Puget Sound aeromagnetic maps and data, *U.S. Geol. Surv Open File Rep. 99–514*. (Available at http://geopubs.wr.usgs.gov/open-file/of99-514.)

Blakely, R. J., R. E. Wells, C. S. Weaver, and S. Y. Johnson (2002), Location, structure, and seismicity of the Seattle fault, Washington, *U.S. Geol. Soc. Am. Bull.*, *114*, 169–177.

Blunt, D. J., D. J. Easterbrook, and N. W. Rutter (1987), Chronology of Pleistocene sediments in the Puget Lowland, Washington, *Bull. Wash. Div. Geol. Earth Resour.*, *77*, 321–353.

Booth, D. B. (1991), Geologic map of Vashon and Maury Islands, King County, Washington, scale 1:24000, *U.S. Geol. Surv. Map MF-2161*, 6 pp.

Booth, D. B. (1994), Glaciofluvial infilling and scour of the Puget Lowland, Washington, during ice-sheet glaciation, *Geology*, *22*, 695–698.

Brocher, T. M., and A. L. Ruebel (1998), Compilation of 29 sonic and density logs from 23 oil test wells in western Washington State, *U.S. Geol. Surv. Open File Rep., 98–249*, 1–60.

Brocher, T. M., T. Parsons, R. J. Blakely, N. I. Christensen, M. A. Fisher, R. E. Wells, and the SHIPS Working Group (2001), Upper crustal structure in Puget Lowland, Washington: Results from the 1998 seismic hazards investigation in Puget Sound, *J. Geophys. Res.*, *106*, 13,541–13,564.

Bucknam, R. C., E. Hemphill-Haley, and E. B. Leopold (1992), Abrupt uplift within the past 1,700 years at southern Puget Sound, Washington, *Science*, *258*, 1611–1614.

Calvert, A. J., M. A. Fisher, and the SHIPS Working Group (2001), Imaging the Seattle fault zone with high-resolution seismic tomography, *Geophys. Res. Lett.*, *28*, 2337–2340.

Calvert, A. J., M. A. Fisher, S. Y. Johnson, and the SHIPS Working Group (2003), Along-strike variations in the shallow seismic velocity structure of the Seattle fault zone: Evidence for fault segmentation beneath Puget Sound, *J. Geophys. Res.*, *108*(B1), 2005, doi:10.1029/2001JB001703.

Chemenda, A., S. Lallemand, and A. Bokun (2000), Strain partitioning and interplate friction in oblique subduction zones; constraints provided by experimental modeling, *J. Geophys. Res.*, *105*, 5567–5581.

Christie-Blick, N., and K. T. Biddle (1985), Deformation and basin formation along strike-slip faults, in *Strike-Slip Deformation, Basin Formation, and Sedimentation*, edited by K. T. Biddle and N. Christie-Blick, *Spec. Publ. Soc. Econ. Paleontol. Mineral.*, *37*, 1–34.

Croot, D. G. (1988), *Glaciotectonic Forms and Processes*, 212 pp., A. A. Balkema, Brookfield, Vt.

Danes, Z. F., M. M. Bonno, E. Brau, W. D. Gilham, T. F. Hoffman, D. Johansen, M. H. Jones, B. Malfait, J. Masten, and G. O. Teague (1965), Geophysical investigations of the southern Puget Sound area, Washington, *J. Geophys. Res.*, *70*, 5573–5579.

Davies, T. A., T. Bell, A. K. Cooper, H. Josenhans, L. Polyak, A. Solheim, M. S. Stoker, and J. A. Stravers (1997), *Glaciated Continental Margins: An Atlas of Acoustic Images*, 315 pp., Chapman and Hall, New York.

Dethier, D. P., F. Pessl Jr., R. F. Keuler, M. A. Balzarini, and D. R. Pevear (1995), Late Wisconsin glaciomarine deposition and isostatic rebound, northern Puget Lowland, Washington, *Geol. Soc. Am. Bull.*, *107*, 1288–1303.

Easterbrook, D. J. (1968), Pleistocene stratigraphy of Island County, *Wash. Dep. Water Resourc. Water Supply Bull.*, *25*, *I*, 1–34.

Easterbrook, D. J. (1994), Chronology of pre-late Wisconsin Pleistocene sediments in the Puget Lowland, Washington, in *Regional Geology of Washington State*, edited by R. Lasmanis and E. S. Cheney, *Bull. Wash. Div. Geol. Earth Resour.*, *80*, 191–206.

Fabbri, O., and M. Fournier (1999), Extension in the southern Ryukyu arc (Japan): Link with oblique subduction and back arc rifting, *Tectonics*, *18*, 486–497.

Finn, C. (1990), sical constraints on Washington convergent margin structure, *J. Geophys. Res.*, *95*, 19,533–19,546.

Finn, C., W. M. Phillips, D. L. Williams (1991), Gravity anomaly and terrain maps of Washington, scale 1:500000 and 1:1,000,000, *U.S. Geol. Surv. Geophys. Invest. Map, GP-988*.

Fisher, M. A., and Expedition Participants (1999), Seismic survey probes urban earthquake hazards in Pacific Northwest, *Eos Trans. AGU*, *80*(2), 13, 16–17.

Fitch, T. J. (1972), Plate convergence, transcurrent faults, and internal deformation adjacent to southeast Asia and the western Pacific, *J. Geophys. Res.*, *77*, 4432–4460.

Frankel, A. D., C. S. Mueller, T. A. Barnhard, D. M. Perkins, E. V. Leyendecker, N. C. Dickman, S. L. Hanson, and M. G. Hopper (1996), National seismic hazards maps, June 1996 documentation, *U.S. Geol. Surv. Open File Rep., 96–532*. (Available at http://geohazards.cr.usgs.gov/eq/.)

Frankel, A. D., et al. (2002), Documentation for the 2002 update of the National seismic hazard maps, *U.S. Geol. Surv. Open File Rep., 02-420*. (Available at http://geohazards.cr.usgs.gov/eq/.)

Freymueller, J. T., J. N. Kellogg, and V. Vega (1993), Plate motions in the north Andean region, *J. Geophys. Res.*, *98*, 21,853–21,863.

Geist, E. L., J. R. Childs, and D. W. Scholl (1988), The origin of summit basins of the Aleutian Ridge; implications for block rotation of an arc massif, *Tectonics*, *7*, 327–341.

Gower, H. D., J. C. Yount, and R. S. Crosson (1985), Seismotectonic map of the Puget Sound region, Washington, scale 1:250,000, *U.S. Geol. Surv, Misc. Invest. Map, I-1613*.

Gradstein, F. M., and J. G. Ogg (1996), A Phanerozoic time scale, *Episodes*, *19*, 3–4.

Haeussler, P. J., and K. P. Clark (2000), Preliminary geologic map of the Wildcat Lake 7. 5′ quadrangle, Kitsap and Mason Counties, Washington, scale 1:24000, *U.S. Geol. Surv Open File Rep., 00-356*.

Hagstrum, J. T., D. B. Booth, K. G. Troost, and R. J. Blakely (2002), Magnetostratigraphy, paleomagnetic correlation, and deformation of Pleistocene deposits in the south central Puget Lowland, Washington, *J. Geophys. Res.*, *107*(B4), 2079, doi:10.1029/2001JB000557.

Harding, T. P. (1985), Seismic characteristics and identification of negative flower structures, positive flower structures, and positive structural inversion, *AAPG Bull.*, *69*, 582–600.

Hashimoto, M., and D. D. Jackson (1993), Plate tectonics and crustal deformation around the Japanese Islands, *J. Geophys. Res.*, *98*, 16,149–16,166.

Jarrard, R. D. (1986), Terrane motion by strike-slip faulting of forearc slivers, *Geology*, *18*, 780–783.

Johnson, S. Y., C. J. Potter, and J. M. Armentrout (1994), Origin and evolution of the Seattle basin and Seattle fault, *Geology*, *22*, 71–74.

Johnson, S. Y., C. J. Potter, J. M. Armentrout, J. J. Miller, C. Finn, and C. S. Weaver (1996), The southern Whidbey Island fault, an active structure in the Puget Lowland, Washington, *Geol. Soc. Am. Bull.*, *108*, 334–354.

Johnson, S. Y., S. V. Dadisman, J. R. Childs, and W. D. Stanley (1999), Active tectonics of the Seattle fault and central Puget Lowland: Implications for earthquake hazards, *Geol. Soc. Am. Bull.*, *111*, 1042–1053.

Johnson, S. Y., S. V. Dadisman, D. C. Mosher, R. J. Blakely, and J. R. Childs (2001), Active tectonics of the Devils Mountain fault and related structures, northern Puget Lowland and eastern Strait of Juan de Fuca region, Pacific Northwest, *U.S. Geol. Surv. Prof. Pap.*, *1643*, 46 pp., 2 plates.

Johnson, S. Y., et al. (2003), Maps and data from a trench investigation of the Utsalady Point fault, Whidbey Island, Washington, *U.S. Geol. Surv. Misc. Invest. Map 2420*, 1 plate.

Jones, M. A. (1996), Thickness of unconsolidated deposits in the Puget Sound Lowland, Washington and British Columbia, *U.S. Geol. Surv. Water Resour. Invest. Rep., 94-4133*.

Khazaradze, G., A. Qamar, and H. Dragert (1999), Tectonic deformation in western Washington from continuous GPS measurements, *Geophys. Res. Lett.*, *26*, 3153–3156.

Lallemand, S., L. Char-Shine, S. Dominguez, P. Schnurle, and J. Malavieille (1999), Trench-parallel stretching and folding of forearc basins and lateral migration of the accretionary wedge in the southern Ryukyus: A case of strain partition caused by oblique convergence, *Tectonics*, *18*, 231–247.

Lees, J. M., and R. S. Crosson (1990), Tomographic imaging of local earthquake delay times for 3-D velocity variation in western Washington, *J. Geophys. Res.*, *95*, 4763–4776.

Mahan, S. A., D. B. Booth, and K. G. Troost (2000), Luminescence dating of glacially derived sediments—A case study for the Seattle mapping project, *Geol. Soc. Am. Abstr. Programs*, *32*, A27.

Mazotti, S., H. Dragert, and R. D. Hyndman (2002), N-S shortening across the Olympic Mountains and Puget Sound evidenced by GPS, *Geol. Soc. Am. Abstr. Programs*, *34*, A90.

McCaffrey, R., M. D. Long, C. Goldfinger, P. C. Zwick, J. L. Nabelek, C. K. Johnson, and C. Smith (2000a), Rotation and plate locking at the southern Cascadia subduction zone, *Geophys. Res. Lett.*, *27*, 3117–3120.

McCaffrey, R., P. C. Zwick, Y. Block, L. Prawirodirdjo, J. F. Genrich, C. W. Stevens, S. S. O. Puntodewo, and C. Subarya (2000b), Strain partitioning during oblique plate convergence in northern Sumatra: Geodetic and seismologic constraints and numerical modeling, *J. Geophys. Res.*, *105*, 28,363–28,376.

McClay, K. R. (1992), Glossary of thrust tectonic terms, in *Thrust Tectonics*, edited by K. R. McClay, pp. 419–433, Chapman and Hall, New York.

Miller, M. M., D. J. Miller, C. M. Rubin, H. Dragert, K. Wang, A. Qamar, and C. Goldfinger (2001), GPS-determination of along-strike variation in Cascadia margin kinematics: Implications for relative plate motion, subduction zone coupling, and permanent deformation, *Tectonics*, *20*, 161–176.

Nelson, A. R., et al. (2002), Field and Laboratory data from an earthquake history study of the Toe Jam Hill fault, Bainbridge Island, Washington, *U.S. Geol. Surv. Open File Rep., 02–60*, 37 pp., 2 plates.

Nelson, A. R., S.Y., Johnson, H. M. Kelsey, B. L. Sherrod, R. E. Wells, K. Okumura, L.-A. Bradley, and R. Bogar (2003a), Field and Laboratory data form an earthquake history study of the Waterman Point fault, Kitsap County, Washington, *U.S. Geol. Surv. MF-Map 2423*, 1 plate.

Nelson, A. R., S. Y. Johnson, H. M. Kelsey, R. E. Wells, B. L. Sherrod, S. K. Pezzopane, L. Bradley, and R. D. Koehler III (2003b), Late Holocene earthquakes on the Toe Jam Hill fault, Seattle fault zone, Bainbridge Island, Washington, *Geol. Soc. Am. Bull.*, *115*, 1388–1403.

Pratt, T. L., S. Y. Johnson, C. J. Potter, and W. J. Stephenson (1997), Seismic reflection images beneath Puget Sound, western Washington State: The Puget Lowland thrust sheet hypothesis, *J. Geophys. Res.*, *102*, 27,469–27,490.

Sangree, J. B., and J. M. Widmier (1977), Seismic stratigraphy and global changes in sea level, part 9: Seismic interpretation of clastic depositional facies, in *Seismic Stratigraphy: Applications to Hydrocarbon Exploration*, edited by C. E. Payton, *AAPG Mem.*, *26*, 165–184.

Sceva, J. E. (1957), Geology and ground-water resources, Kitsap County, Washington, *U.S. Geol. Surv. Water Supply Pap.*, *1413*, 178 pp., 3 plates.

Schneider, C. L., C. Hummon, R. S. Yeats, and G. L. Huftile (1996), Structural evolution of the northern Los Angeles basin, *Tectonics*, *15*, 341–355.

Shaw, J. H., and J. Suppe (1994), Active faulting and growth folding in the eastern Santa Barbara Channel, California, *Geol. Soc. Am. Bull.*, *106*, 607–626.

Sherrod, B. L., R. C. Bucknam, and E. B. Leopold (2000), Holocene relative sea level changes along the Seattle fault at Restoration Point, Washington, *Quat. Res.*, *54*, 384–393.

Sherrod, B. L., T. M. Brocher, and R. C. Bucknam (2002), Asynchronous land-level change along the Tacoma fault in A. D. 800–1200 (abstract), *Seismol. Res. Lett.*, *73*, 240.

Sherrod, B. L., T. M. Brocher, C. S. Weaver, R. C. Bucknam, R. J. Blakely, H. M. Kelsey, A. R. Nelson, and R. Haugerud (2003), Holocene fault scarps near Tacoma, Washington, *Geology*, in press.

Stoker, M. S., J. B. Pheasant, and H. Josenhans (1997), Seismic methods and interpretation, in *Glaciated Continental Margins: An Atlas of Acoustic Images*, edited by T. A. Davies et al., pp. 9–26, Chapman and Hall, New York.

Suppe, J. (1983), Geometry and kinematics of fault-bend folding, *Am. Sci., J.*, *282*, 684–721.

Suppe, J., and D. A. Medwedeff (1990), Geometry and kinematics of fault-propagation folding, *Ecologae Geol. Helv.*, *83*, 409–454.

Suppe, J., G. T. Chou, and S. C. Hook (1992), Rates of folding and faulting determined from growth strata, in *Thrust Tectonics*, edited by K. R. McClay, pp. 105–121, Chapman and Hall, New York.

Tabor, R. W., and W. M. Cady (1978), Geologic map of the Olympic Peninsula, Washington, scale 1:125,000, *U.S. Geol. Surv. Misc. Invest. Map, I-994*.

Tabor, R. W., V. A. Frizzell Jr., D. B. Booth, R. B. Waitt Jr., J. T. Whetten, and R. E. Zartman (1993), Geologic map of the Skykomish River 30 × 60 minute quadrangle, Washington, scale 1:100,000, *U.S. Geol. Surv. Misc. Invest. Map, I-1963*.

ten Brink, U. S., P. C. Molzer, M. A. Fisher, R. J. Blakely, R. C. Bucknam, T. Parsons, R. S. Crosson, and K. C. Creager (2002), Subsurface geometry and evolution of the Seattle fault zone and the Seattle basin, Washington, *Bull. Seismol. Soc. Am.*, *92*, 1737–1753.

Tréhu, A. M., I. Asudeh, T. M. Brocher, J. Luetgert, W. D. Mooney, J. L. Nabelek, and Y. Nakumura (1994), Crustal architecture of the Cascadia forearc, *Science*, *266*, 237–243.

Troost, K. G. (1999), The Olympia nonglacial interval in the southcentral Puget Lowland, Washington, M.S. thesis, 122 pp., Univ. of Wash., Seattle.

Troost, K. G. (2002), Summary of the Olympia nonglacial interval (MIS 3) in the Puget Lowland, Washington, *Geol. Soc. Am. Abstr. Programs*, *34*, A-109.

Van Der Meer, J. J. M. (1987), *Tills and Glaciotectonics*, 270 pp., A.A. Balkema, Brookfield, Vt.

Walsh, T. J., M. A. Korosec, M. W. Phillips, F. J. Logan, and H. W. Schasse (1987), Geologic map of Washington-southwest quadrant, scale 1:250,000, *Wash. Div. Geol. Earth Resour. Geol. Map, GM-34*.

Washington Public Power Supply System (1981), Regional geologic map, scale 1:1,000,000, in *WPPSS Nuclear Project No. 2—Final Safety Analysis Report, Amendment 18*, *WPPSS Docket 50–397*, *2*.

Wells, R. E., C. S. Weaver, and R. J. Blakely (1998), Fore-arc migration in Cascadia and its neotectonic significance, *Geology*, *26*, 759–762.

Whetten, J. T., P. I. Carroll, H. D. Gower, E. H. Brown, and F. Pessl Jr. (1988), Bedrock geologic map of the Port Townsend 30- by 60-minute quadrangle, Puget Sound Region, Washington, scale 1:100,000, *U.S. Geol. Surv. Misc. Invest. Map, I-1198-G*.

Wilson, J. R., M. J. Bartholomew, and R. J. Carson (1979), Late Quaternary faults and their relationship to tectonism in the Olympic Peninsula, Washington, *Geology*, *7*, 235–239.

Yount, J. C., and H. D. Gower (1991), Bedrock geologic map of the Seattle 30′ by 60′ quadrangle, Washington, scale 1:100000, *U.S. Geol. Surv. Open File Rep., 91–147*, 37 pp., 4 plates.

Yount, J. C., G. R. Dembroff, and G. M. Barats (1985), Map showing depth to bedrock in the Seattle 30′ by 60′ quadrangle, Washington, scale 1:100000, *U.S. Geol. Surv. Misc. Field Stud. Map, MF-1692*.

Yu, G., S. G. Wesnowsky, and G. Ekstrom (1993), Slip partitioning along major convergent plate boundaries, *Pure Appl. Geophys.*, *140*, 183–210.

R. J. Blakely and M. A. Fisher, U.S. Geological Survey, MS 977, 345 Middlefield Road, Menlo Park, CA 94025, USA. (blakely@usgs.gov; mfisher@usgs.gov)

S. V. Dadisman, U.S. Geological Survey, 600 4th Street South, St. Petersburg, FL 33701, USA. (sdadisman@usgs.gov)

S. Y. Johnson, U.S. Geological Survey, Pacific Science Center, 400 Natural Bridges Drive, Santa Cruz, CA 95060, USA. (sjohnson@usgs.gov)

W. J. Stephenson, U.S. Geological Survey, MS 966, P.O. Box 25046, Denver, CO 80225, USA. (stephens@usgs.gov)